Overview of the Monsoon-influenced Ayeyarwady River delta, and delta shoreline mobility in response to changing fluvial sediment supply

Edward J. Anthony, Manon Besset, Philippe Dussouillez, Marc Goichot, Hubert Loisel

Overview of the Monsoon-influenced Ayeyarwady River delta, and delta shoreline mobility in response to changing fluvial sediment supply

Edward J. Anthony[a,b], Manon Besset[a,c], Philippe Dussouillez[a], Marc Goichot[d], Hubert Loisel[e]

[a]*Aix Marseille University, CNRS, IRD, INRA, Coll France, CEREGE, Aix-en-Provence, France*

[b]*USR LEEISA, CNRS, Cayenne, French Guiana*

[c]*University of Montpellier, Geoscience Montpellier, Montpellier, France*

[d]*Lead, Water, WWF Greater Mekong Programme, 14B Ky Dong Street, Ward 9, District 3, Ho Chi Minh, Viet Nam*

[e]*Laboratoire d'Océanologie et de Géosciences, Université du Littoral-Côte-d'Opale, Université Lille, CNRS, UMR 8187, LOG, 32 avenue Foch, Wimereux, France*

Abstract

A morpho-sedimentary analysis of the Ayeyarwady delta shoreline was conducted based on a field mission in Myanmar in November 2016 and interpretation of satellite images spanning the period 1974-2019. These analyses were complemented by data on land-to-water conversion and vice versa within a 2 km-wide coastal fringe, and on MERIS-derived seasonal and decadal-scale evolution of suspended particulate matter (SPM) off the delta. The objectives were to: (1) characterize the 450 km-long delta shoreline and coastal sediment transport pathways, (2) define the shoreline status (stability, erosion, accretion), and (3) identify potential causes of shoreline change and the future outcome of this status in terms of delta vulnerability. The delta shoreline was characterized on the basis of qualitative alongshore tidal, wave-energy, and sediment grain-size patterns (muddy, sandy or a mixture of both), and morphology (sandy beaches and mudflats). The deltaic coast exhibits a mixed wave-and-tide-dominated morphology and comprises a western sector characterized by four of the five main distributary mouths separating inter-distributary plains bounded by low

overwash-influenced beaches devoid of aeolian dunes. The eastern sector, in the Gulf of Martaban, is embayed, much less prograded and bounded by dominantly muddy shores. This simple shoreline dichotomy reflects the overarching alongshore sediment redistribution and storage patterns that have accompanied the growth of the delta, resulting in the two facies: sand dominantly retained in the western sector where the multiple distributary mouths have constrained potential alongshore sand transport by low- to moderate-energy monsoon-generated southwesterly waves, and mud transported by the regional monsoon-influenced coastal shelf circulation towards the eastern sector. The recent multi-decadal shoreline mobility in the Ayeyarwady delta points to the influence of fluvial sediment supply on these two facies. Between 1974 and 2019, 49% of the delta's shoreline underwent erosion, mainly affecting the sandy beaches in the western sector, whereas shoreline accretion is still prevalent along the large inter-distributary plain east of Yangon, where coastal mud preferentially accumulates in the Gulf of Martaban. We attribute erosion to reduced river sand supply generated by dams and by massive in-channel sand mining upstream of the delta, exacerbated by important channel dredging. Large-scale deforestation resulting from land-use changes (agriculture and mining) in the Ayeyarwady catchment are probably contributing to enhanced fine-grained sediment supply to the delta plain and the coast, as reflected by the relative stability of coastal SPM over a decade (2002-2012) and continued deposition in the accreting eastern sheltered part of the delta. The coastal sediment balance will be further impacted in the future if planned dams are constructed. Without proper sediment management, notably a significant reduction or prohibition of in-channel sand mining, the sandy beaches that armour the wave-exposed western sector of the delta will continue to erode, resulting in increased potential exposure of the delta to cyclones and sea-level rise.

Keywords: monsoon-influenced delta; delta erosion; river sediment supply; coastal suspended particulate matter; Ayeyarwady, Gulf of Martaban

Highlights

1. The monsoon-influenced Ayeyarwady delta shows prograded west and embayed east sectors

2. The sandy west sector eroded between 1974 and 2019 despite proximity of delta distributaries

3. In contrast, active mud-trapping in the eastern sector contributes to significant progradation

4. Contrast reflects influence of changing fluvial sand and mud supply induced by human activities

5. Sand supply is reduced by channel extraction and fine-grained supply enhanced by deforestation

1. Introduction

Many deltas are becoming economically and environmentally vulnerable and their physical and biological resilience declining as a result of human activities (Brondizio et al., 2016; Seijger et al., 2016; Hagenlocher et al., 2018). Increased vulnerability and loss of resilience occur as a result of reduced sediment flux from rivers and various other modifications caused by human interventions (Ericson et al., 2007; Syvitski and Saito, 2007; Syvitski et al., 2009; Evans, 2012; Besset et al., 2019; Grill et al., 2019). These conditions are aggravated by climate change and sea-level rise. The Ayeyarwady River, in Myanmar (Fig. 1), is increasingly affected by problems related to water and sediment management (WWF, 2018) that are affecting the delta (Anthony et al., 2017). The Ayeyarwady delta is an important component of the developing economy of Myanmar, the largest country (676,600 km^2) in mainland Southeast Asia. Myanmar is heavily reliant on the economic advantages provided by the river and its delta, and is also among the 15 nations that, together, account for 80% of the world's population exposed to river (including delta) flood risk world-wide (Ward et al., 2013; Winsemius et al., 2013). This situation is of particular concern to the disproportionately large river delta (Fig. 2A). As in most developing countries, population growth in Myanmar has been extremely rapid, exacerbating exposure to the risks of river flooding, cyclones, and coastal erosion. The Ayeyarwady delta is particularly populous with over 15 million people, and registered an increase of nearly 150% in about 30 years (Brakenridge et al., 2017). The advantages provided by the delta as a home to millions of people and as Myanmar's food basket could be seriously offset by massive on-going in-channel aggregate extractions and, in the coming years, by the impacts of numerous

projected dams (Hennig, 2016; Taft and Evers, 2016) that could further stifle sediment supply (WWF, 2018).

Compared to most Asian and Pacific mega-deltas, the knowledge acquired on the Ayeyarwady system is quite sparse, and the morpho-sedimentary dynamics of the delta are still relatively understudied, notwithstanding a few recent efforts geared at shoreline changes (Hedley et al., 2010; Anthony et al., 2017), flood impact (Brakenridge et al., 2017), shoreline response to cyclone activity (Besset et al., 2017), and Holocene evolution (Giosan et al., 2018). Acquiring data on this large delta should be an important objective with high relevance for the future development of Myanmar. The delta, like the catchment of which it is a part, crystallizes factors related to environment and water management, climate, economic and social development, land-use changes (Taft and Evers, 2016), as well as the sediment issue, which is particularly pertinent to delta sustainability.

The aim of this paper is to characterize the 450 km-long delta shoreline and its coastal sediment transport pathways, define the recent to current shoreline status (stability, erosion, accretion), and identify potential causes of shoreline change and the future outcome of this status in terms of delta vulnerability. In particular, the link between changing fluvial sediment supply, increasingly influenced by a variety of drivers, notably anthropogenic, and shoreline mobility, forms the overarching discussion theme.

2. The Ayeyarwady River and delta: a general overview

The Ayeyarwady has its source in the eastern Himalaya and lies in a zone of active tectonics in the collision zone between the Indian and Eurasian Plates (Wang et al., 2014), a context favourable to large fluvial water and sediment discharges. The river's catchment covers 404,100 km^2 and comprises three large tributaries, the Chindwin, Shweli, and Myitnge rivers (Fig. 1), separated in the northern reaches by alluvial floodplains. The downstream end of this drainage system has formed a large delta (Fig. 2A) in the Andaman Sea that merges eastward with the mouth of the smaller catchment of the Sittaung River (48,100 km^2). The Ayeyarwady delta and the contiguous coastal deposits of the Sittaung have formed 20,570 km^2 of low, fertile plain (Brakenridge et al., 2017). Although only 23rd in world catchment size rankings, the Ayeyarwady delta, with its Sittaung extension, ranks 11th in size among the deltas of the world (Coleman and Huh, 2004).

Overviews on the hydrology, geomorphology, sedimentology, and flood risks of the Ayeyarwady have been provided recently by van der Velden (2015), Brakenridge et al. (2017), and WWF (2018). The Ayeyarwady catchment experiences a tropical seasonal monsoon climate with rainfall concentrated in the hot humid months of May to October (Indian monsoon) as southwest winds blow northeastwards across the Bay of Bengal in the wake of the northward movement of the Intertropical Convergence Zone (ITCZ). In contrast, dry northwest winds blow from the continent during the cool months of December to March (Asian monsoon). The mean annual rainfall across the delta ranges from 2000 to 3000 mm, but other parts of the river's catchment experience up to 6000 mm of rainfall (Frenken, 2012). Tropical cyclonic storms make landfall in Myanmar between May and October, generate heavy rainfall and severe flooding (Brakenridge et al., 2017), and their frequency seems to be affected by the Pacific Decadal Oscillation (PDO) (Haggag et al., 2010).

The present Ayeyarwady deltaic complex (Fig. 2A) developed in a confined setting between north-south-aligned bedrock ridges (Western Hills and Eastern Hills) as a bay-head delta (Fig. 1), a common development setting for many river deltas worldwide (Anthony, 2015, 2016). Embayed settings are particularly favourable to the trapping of fluvial (and marine) sediments, as wave reworking, redistribution, and dispersal are commonly hampered. The delta coast, including the Gulf of Martaban (Gulf of Moutama), is adjacent to a relatively shallow shelf, and with a maximum depth of only about 50 m, composed of sediments deposited by the Ayeyarwady, the Sittaung, and the Salween (324,000 km^2) (Ramaswamy et al., 2004). The shelf width is about 170 km off the Ayeyarwaddy delta and increases to more than 250 km in the centre of the Gulf of Martaban (Damodararao et al., 2016).

Coastal currents in the Andaman Sea off the delta are mainly governed by the monsoon winds, as well as by Rossby waves triggered by Ekman transport and by Equatorial Kelvin waves (Suwannathatsa et al., 2012). Current flows are dominantly alongshore from west to east, and this is important in the alongshore mobility of fine-grained sediment exiting from the multiple distributary mouths in the west, as discussed below. The wave regime is characterized by monsoon wind waves of moderate fetch (wave periods of 8-12 s with a mean of about 10 s) generated in the Andaman Sea by the southwesterly winds, and thus, almost exclusively from a southwest direction (Fig. 2B), but with a marked seasonal variability in height (Anthony et al., 2017). Waves are highest in July (mean values of up to 2

m) at the peak of the rainy Indian monsoon season. Their heights diminish during the dry season when the influence of southwest monsoon winds becomes attenuated due to the southward migration of the ITCZ. Maximum wave heights can reach 5 m during cyclones. Figure 2C shows a map of the dominant M2 tidal amplitude in the Andaman Sea and a 12-month extract of the tidal record from an offshore tide gauge in the delta (see location in Fig. 2A) for 2018. According to Kravtsova et al. (2009), the mean tidal range along the western shores of the delta is 3.0 m and about 3.2 m along the eastern shores. This data source further indicates that the tidal range during spring and neap tides along the western extremity of the delta are 2.2 m and 1.8 m, respectively, but up to 5.7 m and 4.0 m, respectively, along the eastern extremity of the delta off the mouth of the Sittaung. These values are similar to those of Volker (1966) who identified spring and neap tides at the eastern periphery of the Ayeyarwady delta amounting to 5.8 m and 4.0 m, respectively. These ranges attain 5.1 m and 3.5 m, respectively, in Yangon located 72 km from the sea. Spring-tide influence extends almost 300 km inland to the apex of the delta (Hedley et al., 2010). Tropical cyclones, thoroughly reviewed by Brakenridge et al. (2017), may generate strong coastal surges, resulting in significant damage periodically (Dube et al., 2010). Tropical Cyclone Nargis (2-4 May 2008), a category 5 event just prior to landfall in Myanmar, is the latest and strongest meteorological event to have affected the delta in historic times, causing the worst natural disaster in the recorded history of Myanmar (Fritz et al., 2009), and massive shoreline retreat (Besset et al., 2017).

According to data collated by Kravtsova et al. (2009), the mean fluctuation of sea level in the Andaman Sea within a year is about 8 cm. Sea level is slightly higher during the rainy season than the dry season due to the impact of river runoff. Seasonal sea-level fluctuations do not therefore play a significant role in the coastal hydrodynamic regime, which is dominated by winds, wind waves and moderately large tides.

In terms of the dominant marine processes acting to shape the delta's shoreline, the Ayeyarwady comes out as an example of a mixed wave-and-tide-dominated system in the commonly used classification system of Galloway (1975). Five main distributary mouths have developed downstream of the main-stem Chindwin and Ayeyarwady channels to convey the high water and sediment flux to the prograding delta in its western sector, where four main distributaries debouch (the fifth main one corresponds to the Yangon distributary in the eastern sector, Fig. 2A). The western sector is more significantly wave-influenced than the

less prograded embayed eastern sector which is more wave-sheltered and essentially composed of open-coast muddy-sandy tidal flats. Wave influence is reflected in the formation of beach-ridge sets in some of the inter-distributary plains, especially the large 'promontory' between sites 7 and 10 (Fig. 2A), indicating that this western sector has formed a depocentre for sand supplied by the rivers (Anthony et al., 2017; Giosan et al., 2018; Kuehl et al., 2019). Wave influence in this sector is both a cause and consequence of a more prograded sector of coast (Fig. 1). Progradation has culminated in a more protruding delta lobe in this sector relative to the southwesterly monsoon waves, which enhances the efficacy of wave-reworking of the shoreline in the context of a moderate tidal range. As in other deltas, the progressive growth and seaward protrusion of the delta have been tantamount to increasing wave influence (Anthony, 2015). However, this influence has been moderated by the presence of the multiple distributary mouths, as well as by tidal amplification in the embayed eastern sector of the delta. Beach-ridge development has been both more recent (Giosan et al., 2018) and more limited in the eastern sector of the delta, probably sourced from the Yangon tributary.

The distributary mouths have remained relatively fixed in the western sector of the delta, as suggested by radiometric ages from beach-ridge deposits (Giosan et al., 2018). The inception and development of these distributaries appear to stem from channel bifurcations (Jerolmack, 2009) around distributary mouth bars, as has been proposed for the multiple mouths of the Mekong River delta (Tamura et al., 2012). The increase in tidal range eastward is the outcome of amplification of the tidal wave propagating over the shallow Andaman shelf and Gulf of Martaban embayment. The shallow shelf itself is a product of pronounced river, coastal and marine sedimentation through geological times that has produced the thick sedimentary deposits of the Central Burma Basin down to the Andaman shelf (Rodolfo, 1969b).

3. Fluvial water and sediment discharge to the coast and alongshore transport

The disproportionately large size of the Ayearwady delta relative to the size of its river catchment reflects a favourable combination of a high river sediment supply related to an active tectonic context, a steep upper catchment topography, high monsoon rainfall, the confined bay-head morphological setting of delta growth between bedrock promontories, and the moderate hydrodynamic conditions of the Andaman Sea (Anthony et al., 2017). The

Ayeyarwady river catchment collects nearly 70% of the surface water volume of Myanmar (Kravtsova et al., 2009). The combined discharge of the Ayeyarwady and Chindwin Rivers at Chauk (Fig. 1) ranges from about 1500 m^3/s to about 30,000 m^3/s (van der Velden, 2015), and shows a strongly seasonal monsoon pattern (Stamp, 1940). Robinson et al. (2007) calculated, from data collected between 1969 and 1996 at Pyay (Fig. 1), an annual water discharge of 44,241 km^3 and a sediment discharge to the ocean of 226-364 Mt, concentrated in the rainy season, and among the highest in the world. Using these data, Furuichi et al. (2009) estimated the water discharge (379 $\pm 47.10^9$ Mt/year) and suspended sediment load (325 $\pm$57. Mt/year) for the river upstream of the delta head. These values are similar to those derived by WWF (2018) who also estimated a widely-ranging bedload volume of 7.2 to 34 Mt/year (i.e., about 3 to 15% of the total load). A statistical comparison carried out by Furuichi et al. (2009) with earlier, 19^{th} century data (1871 to 1879), shows a significant decrease in discharge in the last 100 years. Sediment discharge over the last few decades has been strongly affected by anthropogenic pressures in the catchment (WWF, 2018), as discussed later. Shorter-term fluctuations would also be expected from climatic variability. Precipitation in Myanmar is known to be affected by the inter-annual El Niño/Southern Oscillation (ENSO) (Krishnamurthy and Goswami, 2000; Furuichi et al., 2009), by the ENSO counterpart of El Niño (La Niña; equatorial Pacific cold water anomalies) (Rojas et al., 2014; Sein et al., 2015), by the intra-seasonal Madden–Julian Oscillation (Hendon and Salby, 1994), which is a tropical to near-global alternation in atmospheric and oceanic circulation patterns and rainfall, and finally by the Indian Ocean Dipole with which rainfall in Myanmar is negatively correlated, and which notably modulates monsoon rainfall (Ashok et al., 2001). Finally, rates of meltwater, and the frequency of the tropical cyclonic storms that make landfall in Myanmar between May and October, and which are accompanied by exceptionally heavy rainfall (Brakenridge et al., 2017), are deemed to be affected by the Pacific Decadal Oscillation (Haggag et al., 2010). Based on a sediment discharge at Chauk ranging from 165 kg/s in the dry season to 18,000 kg/s at the peak of the Indian monsoon, Kravtsova et al. (2009) calculated the mean water turbidity at the mouths of the Ayeyarwady at approximately 600 g/m^3, which corresponds to relatively high values.

60 ±10% of the total sediment flux downstream is supplied by the Chindwin, the sub-catchment of which is characterized by more readily erodible rocks (Garzanti et al., 2016). It is not clear, however, how water and sediment are apportioned among the five major and

246 various smaller distributaries of the Ayeyarwady. Sand constitutes much of the shoreline in
247 the western sector of the delta (Fig. 2A). There are no data on shoreline sand budgets for the
248 individual beaches bounding the inter-distributary plains. It is clear, from the more advanced
249 progradation of this western sector (Fig. 2A), that the sand supplied by the river to the
250 deltaic shorelines has been sequestered in this sector, possibly throughout the development
251 of the delta.

252 Figure 3A shows 10-year (2002-2012) averaged suspended particulate matter (SPM)
253 concentrations offshore of the delta, compiled from the *GlobCoast* MERIS satellite
254 (http://sextant.ifremer.fr/en/geoportail/sextant). The data were generated through a
255 combination of the Polymer algorithm (Steinmetz et al., 2011) adapted for coastal waters
256 (Loisel et al., 2016) and the SPM algorithm of Han et al. (2016). We assume that these
257 concentrations dominantly reflect fine-grained terrestrial inputs to the coastal sea, an
258 assumption supported by analysis of SPM concentrations for 2008 prior to, in the course of,
259 and following Cyclone Nargis in May 2008 (Besset et al., 2017).

260 The pattern depicted by the *GlobCoast* data is very similar to that derived by
261 Matamin et al. (2015). The seasonal SPM pattern does not strictly adhere to the seasonal
262 rainfall regime, as depicted by water levels in the river close to the delta at Pyay and
263 Hinthada (Fig. 3B), as one would expect a significant increase during the rainy Indian
264 monsoon months (May–October) and a decrease in the dry-season Asian monsoon
265 (December–March). The pattern is strongly influenced by lag effects, given the size of the
266 Ayeyarwady catchment, and, in the offshore zone, by marked cross-shore and alongshore
267 spatial variations. The Indian monsoon is characterized by offshore displacement of the SPM
268 plume starting in May, with a clear banding from the coast to the offshore (Fig. 3A). This
269 stronger offshore displacement, which largely reflects spread of mud under the strong
270 outgoing fluvial jets at the distributary mouths, prevails until January, as the water discharge
271 diminishes during the dry season. However, the strong offshore concentration zone appears
272 to attain a peak in June before waning significantly in July and the remaining rainy season
273 months. This could suggest that offshore SPM concentrations increase rapidly at the start of
274 the rainy season under favorable conditions of coastal supply as river liquid discharge
275 increases in the distributary channels, prior to overbank flooding of the river flood plain and
276 the delta plain. The concentrations then diminish as these terrestrial units sequester a

significant part of the suspension-load supply with the rise in river level and widespread rainy-season flooding.

The alongshore spatial pattern shows that a significant fraction of the mud discharged by the Ayeyarwady into the sea in the western distributary-mouths sector during the Indian monsoon is transported by the regional coastal currents towards the Gulf of Martaban, where the SPM concentrations are highest (Fig. 3A). Here, further trapping of mud debouching from the Sittaung (Fig. 1) occurs. This eastward regional SPM transport pattern is in agreement with the finding of various authors who identified high mud concentrations in the Gulf of Martaban (Rodolfo, 1969a; Ramaswamy et al., 2004; Rao et al., 2005; Matamin et al., 2015; Damodararao et al., 2016; Kuehl et al., 2019). Matamin et al. (2015) and the *GlobCoast* data also show high dry-season concentrations in this eastern part of the delta (Fig. 3A), in agreement with the observations of these authors. These high dry-season concentrations may also reflect some degree of mud resuspension by the strong tidal currents in this macrotidal part of the gulf. The Andaman Sea has been described as highly turbid, and clastic mud is burying carbonate deposits consisting of molluscan fragments and foraminifera tests on the delta shelf, leading to a vertical depositional rate in that area of about 200 cm in 1000 years (Rodolfo, 1969a, 1969b). According to Rodolfo (1969a), and more recently Rao et al. (2005), a small amount of mud reaches the Andaman Basin through the Martaban Canyon, and river-derived mud is not accumulating in the western part of the shelf fronting the delta.

3. Methodology

3.1. Field reconnaissance and alongshore sediment sampling

A field mission aimed at ground-truthing shoreline characteristics (morphology, sedimentology, presence and type of vegetation, qualitative observations of bedforms, and shoreline dynamics), and collection of sand-rich samples for grain-size analysis was conducted in November 17-22, 2016. This mission consisted essentially of reconnaissance work and visits to 17 sites from east to west along the delta shoreline (Fig. 2A). The choice of the sites was based on access permission from the Myanmar administrative authorities and on accessibility. A total of 54 sediment samples were collected from 11 sites characterized by sandy beaches (sites 8 to 17 in the western sector of the delta, and sites 6 and 7 transitional to the eastern sector). Four to five samples were collected on a cross-shore

transect from the lower to the upper beach, using observed bedforms or facies changes, where apparent, to delimit sampling zones. No samples were collected between sites 1 and 5 where the foreshore was characterized by mud. All samples were initially homogeneously separated in the laboratory with a sediment inox splitter and dispersed using 0.3% sodium hexametaphosphate as a dispersing agent. The grain-size distribution was measured using a Beckman Coulter LS 13320 laser grain-sizer with a range of 0.04 to 2000 µm. The calculation model uses the Fraunhöfer and Mie theory. For the calculation model, water was used as the medium (RI = 1.33 at 20 °C), a refractive index in the range of that of kaolinite for the solid phase (RI = 1.56), and absorption coefficients of 0.15 for the 780-nm laser wavelength and 0.2 for the polarized wavelengths (Buurman et al., 1996).

3.2. Multi-decadal shoreline changes

Shoreline changes were analyzed using two metrics: (1) shoreline mobility and induced coastal area change over time, and (2) conversion of coastal land into water, or conversion of adjacent coastal water into land. Data on shoreline mobility and area change were obtained from 47 digitized LANDSAT satellite images (60-30 m pixel size) from 1974 to 2019. Following work on similar delta shorelines, such as the Mekong (Anthony et al., 2015; Besset et al., 2019b), we used the mangrove fringe in the muddy mangrove-dominated sectors, and brush or plantation fringe in sandy, beach-dominated sectors as shoreline markers. These shoreline markers were confirmed in the course of the field observations at the 17 site stops covering over 300 km of the delta's shoreline in November 2016 (Fig. 2A). A specific focus was also set on the impact of Tropical Cyclone Nargis in May, 2008 (Besset et al., 2017), which will only be briefly evoked here insofar as it illustrates the increasing vulnerability of the delta.

Shoreline variations were calculated using the *ArcMap* extension module Digital Shoreline Analysis System (*DSAS*), version *5* (Himmelstoss et al., 2018), coupled with *ArcGIS®10.2.2*. Using a relevant cartographic frame (Projection UTM 48N), a baseline B was set about 1 km offshore of the delta shoreline. This baseline was regular enough to: (i) smooth any small-scale alongshore instabilities, and (ii) delineate large-scale geomorphic features such as distributary mouths, capes or bays. We then set up regularly spaced transects normal to the baseline and extending from offshore to 3 km inland. We set up a transect every 100 m alongshore from which shoreline variations between the changing

vegetation line and the inland base line were calculated between the successive sets of LANDSAT images. This distance, chosen as a compromise between quality of the interpretation and the important length of the Ayeyarwady delta shoreline (~ 450 km) was divided by the time in years between the two image dates to generate statistics of shoreline change in *DSAS 5*. Using *ArcGIS®10.2.2*, we further determined surface area differentials between shorelines of different dates to obtain annual area gains and losses. We retained a relatively large uncertainty shoreline change band of ±20 m, which is much more than commonly used in the literature. The reader is referred to Besset et al. (2019a, 2019b) for the complete error computation methodology.

Data downloaded from the global database of Pekel et al. (2016) were used to identify coastal areas converted from land into water and vice versa in the Ayeyarwady delta. The rationale for examining these transformations is that they are a complementary input on multi-decadal shoreline mobility. Land-to-water conversion generally denotes erosion (but also back-shore land-use changes such as the installation of shrimp farms and rice cultivation), whereas water-to-land conversion implies land gain resulting from shoreline accretion (and less commonly from land reclamation, which is non-existent in the coastal fringe of the Ayeyarwady delta). The data from Pekel et al. (2016) are derived for each pixel (30 x 30 m) of LANDSAT satellite images covering a long-trend of 32 years (1984-2015) that smooths out the impact, on land or water extent, of exceptional events such as droughts or floods. In addition to producing a map covering the delta, we calculated the land-to-water and water-to-land changes in a 2 km-wide coastal fringe relative to the 1984 shoreline. This 2-km fringe is well within the bandwidth of change liable to be caused by shoreline erosion (delta land conversion into coastal water) or accretion (coastal water conversion into delta land). The data also show seasonal patterns of conversion for each pixel. Overall, we retained four conversion categories over the 32-year period of observation, following Besset et al. (2019a): (1) new permanent water surfaces (land into permanent water), (2) loss of permanent water (permanent water into land), (3) permanent water into seasonal water, and (4) seasonal water into permanent water. A single category suffices to validate the presence of water. The category representing the year a change is identified is then considered as the first year of change. The category of the last year is always attributed to the last year of observation (October 2014 to October 2015).

4. Results

4.1. Shoreline morphological and grain-size variations

The November 2016 field reconnaissance enabled the identification of a clear west-to-east change in shoreline morphology and sedimentology (summarized in Fig. 2A in terms of two sectors), and embedded in a transition from a wave-and-tide-dominated system in the western, to a more tide-dominated eastern sector. This difference is reflected in both the pattern of long-term delta development and the coastal landforms, briefly summarized in section 2, and grain-size gradients.

The multiple distributary channels in the western sector (sites 7 to 17, Fig. 4) alternate alongshore with inter-distributary plains and their beach-ridge sets, bounded seaward by low sandy beaches (Fig. 5A) that exhibit, in places, a morphology of multiple bars and troughs. The upper beach is commonly characterized by washovers, and the backshore devoid of foredunes. The beaches front wide back-barrier depressions that are bounded landwards by the most recent sets of beach ridges. Generally, in this sand-rich western sector, the low-tide beach exhibits a grain-size fining trend (Fig. 5A1) and is characterized by an abrupt transition to a muddy foreshore (Fig. 5A2) that commonly exhibits mangrove root remains, indicating erosion associated with barrier translation landwards. Between sites 8 and 6, the D_{50} grain-size values decrease significantly, and the percentage of mud increases, indicating the transition towards the mud-dominant foreshores of the eastern sector (sites 1 to 5). East of the mouth of the Yangon distributary, foreshore mud dominates throughout (Fig. 5B1), colonized by mangroves and, in places, tropical salt marshes (Fig. 5B2).

4.2. Multi-decadal shoreline changes

The 450 km of delta shoreline showed a mean overall advance of 9.5 m/yr ± 3.9 m between 1974 and 2019, up from 7.5 m/yr for the period 1974-2015 (Anthony et al., 2017), thus suggesting a mild gain in accretion. This mean rate masks, however, a strong alongshore variability (Fig. 6). Areas of shoreline advance indeed show high rates: a mean of +26 m/year overall, and exceeding 50 m/yr along large stretches and even 100 m/year locally, in the muddy northeast corner of the delta on either side of the mouth of the Yangon tributary where patches of bare low-tide foreshore mud are also visible (Fig. 6). The analysis has not been carried out beyond this accretion zone. Observations of satellite images show that the shoreline in the approaches to the large macrotidal mouth of the Sittaung is

characterized by rapidly changing muddy foreshores that probably correspond to the mud pool accumulating in this corner of the Gulf of Martaban. Shimozono et al. (2019) have highlighted significant morphological changes in the mouth of the Sittaung associated with rapid bank erosion under tidal and fluvial forces.

The overall net retreat rate has been -8 m/yr. Although this rate is well below that of the net advance rate, erosion over the observation period affected, nevertheless, a significant stretch of the delta's shoreline, notably in the western sector of multiple distributary mouths, which are, paradoxically, the delta's main arteries for sediment supply to the coast. Net erosion has prevailed, over the 45-year period of analysis, along 220 km of delta shoreline, i.e., nearly 49%. Erosion has particularly affected the western, distributary-mouth sector (Fig. 6). In order to highlight the temporal trends, an analysis was carried out of shoreline gains and losses in km^2/yr on a time-slice basis (Fig. 7). The western sector has been largely in erosion since 1988, albeit with a progressively attenuated trend. Although this sector has registered very mild gains since 2010, much of this is accounted for by the sandy-muddy transitional zone (between sites 6 and 8, Fig. 2A) to the eastern sector, where one of the two branches of the Yangon distributary debouches (Fig. 6). In this critical western sector, where the delta has prograded most, the current status of the beaches over the latest 2015-2019 period is one of rampant erosion. In contrast to the western sector, the presently accreting northeast sector showed retreat prior to 1988, losing up to 3.35 km^2/year, followed by fluctuations and important advance between 1992 and 2000 related to the formation of a large mud bank that was partially colonized by mangroves and, locally, tropical salt marshes. Shoreline changes since 2000 in the extreme northeast corner of the delta have not been included in the analysis as they show an anomalous erosion hotspot that, in fact, corresponds to in-situ reworking of this mud bank close to the mouth of the Sittaung (Fig. 8). It is important to stress the net coastal land gain of > 25 km^2/yr in this eastern sector since 2015 (Fig. 7).

The land-water (water-land) conversion of the delta is depicted in Fig. 9, together with changes in the 2 km-wide coastal fringe. Conversion of land into water has occurred in large areas of the delta plain, and this pattern also prevails along the 2 km-wide coastal fringe where land-to-water (all categories considered) dominated between 1984 and 2015 (> 70%). This figure largely exceeds that of the shoreline stretch in erosion, but this apparent discrepancy may be due to the choice of a 2 km-wide band. Large stretches of the eroding

western sector of the delta comprise narrow beaches behind which wetlands have appeared that correspond to areas of rice cultivation, but several small areas of water-to-land conversion also appear, and correspond to accreting spits, further discussed below. Conversion of land to water is particularly prominent in the eastern sector (Fig. 9), highlighting some apparent disagreement with the dominant shoreline accretion in this sector (Fig. 6). This inconsistency may, in fact be explained by the tendency for the conversion to include areas that correspond to intertidal shore-detached mud, which may fluctuate considerably in shape and size over time, and with the macrotidal frame. The shoreline is, in contrast, dominated by water-to-land conversion in this sector, reflecting the multi-decadal accretion trend (Fig. 6).

5. Discussion

Delta shorelines are dependent on fluvial sediment supply to balance marine forces of sediment dispersal, subsidence and sea-level rise. There is no simple straightforward relationship between fluvial sediment supply and shoreline mobility, since the latter can also be influenced by various other drivers acting at a variety of timescales (Besset et al., 2019a). However, fluvial sediment supply is the overarching driver of the shoreline mobility of the Ayeyarwady delta, complemented by sediment redistribution processes by monsoon-generated waves and currents along the coast, including regional trapping in the Gulf of Martaban. The simple shoreline dichotomy adopted in this study reflects the overarching alongshore sediment redistribution and storage patterns that have accompanied the growth of the delta and the two resultant facies. Sand is dominantly retained in the western sector, where the multiple distributary mouths have constrained potential alongshore sand transport by low- to moderate-energy monsoon-generated southwesterly waves, and mud transported by the regional monsoon-influenced coastal shelf circulation towards the eastern sector. The recent multi-decadal shoreline mobility in the Ayeyarwady delta points to the influence of fluvial sediment supply on these two facies. According to Rodolfo (1969a), the Ayeyarwady delta prograded at an average rate of 2.5 km in 100 years into the Andaman Sea up to the start of the last quarter of the 20th century. The shoreline erosion pattern drawn out of the satellite data thus shows a significant slow-down in progradation (Figs. 6, 7). These results are in agreement with those of Hedley et al. (2010) who identified a turnaround to erosion starting from 1989.

Although the Ayeyarwady is a high-sediment load river relative to the size of its basin, the erosion that affects the western sector (Fig. 6) is striking, inasmuch as the main sediment sourcing of the delta occurs in this sector of active distributary mouths. Attempting to explain this situation needs taking into account complex mechanisms of catchment-scale sediment release, storage and redistribution strongly mediated by human activities in the last three to four decades, and the propensity for transport of sand and suspension load to the delta's shoreline. To summarize, the western sandy shoreline undergoes erosion whereas the muddy eastern shoreline is accreting more or less strongly, thus calling for an explanation that takes into account the impact, on shoreline mobility, of: (1) the segregation of fine-grained sediment and bedload supplied by the river, (2) the preponderance of sand in the western sector of the delta where the multiple distributary mouths refract waves, leading to immobilization of this fraction in this sector, and (3) the regional-scale transfer, by the hydrodynamic regime, of mud exiting from these distributary mouths towards the Gulf of Martaban.

Fluvial sediment supply in the Ayeyarwady River is influenced by dams, aggregate mining in channels, channel dredging, deforestation, and climate change. Gauging the magnitude of each of these factors at this stage is an impossible task, and the issue is further complicated by differential impacts on bedload and suspended load that can only be grossly outlined, and by the fact that activities that lead to deforestation, such as agriculture and mining on catchment slopes, but also climate change, could actually enhance catchment sediment supply. A 30% drop in sediment supply generated by trapping of the fluvial load behind reservoirs in the Ayeyarwady catchment was calculated by Syvitski and Saito (2007). This is a significant amount. Between 1988 and 2004, for instance the storage capacity of reservoirs on the small tributaries of the Ayeyarwady and Chindwin grew from 2.34 to over 18 km^3 (Myanmar Irrigation Works Department, 2004). Many dams have recently been constructed along the smaller rivers and tributaries, and more are planned for the larger ones (Kattelus et al., 2014; Hennig, 2016; Taft and Evers, 2016; Brakenridge et al., 2017). Assessment of the energy potential of Myanmar identified 92 new large hydropower projects (ADB, 2012), including the controversial Myitsone dam (with a projected potential of 3,600 kW). The project has been suspended by the Government, a decision taken in the broader interests of Myanmar. Data collected by Brakenridge et al. (2017) show that there are currently almost 200 large dams in Myanmar. The impacts of trapping of bedload (sand

501 and gravel) by dams are further aggravated by channel dredging and in-channel mining. The
502 massive scale at which aggregate mining in the Ayeyarwady river channels is practiced has
503 been considered as being more pernicious on the river's bedload supply to the delta than
504 river dams (WWF, 2018). Current volumes of aggregate mining in the river, to the tune of 9
505 Mt (5-6 Mm^3 of sand) and nearly 0.5 Mt (about 0.3 Mm^3 of gravel a year (Fig. 10A), and
506 considered as conservative estimates by WWF (2018), must constitute a significant
507 proportion of the annual bedload supply by the fluvial system, and the true values, are, in
508 fact, likely to be much higher. In addition to aggregate mining, dredging has also been
509 carried out on a large scale in the river channels. Data collated by WWF (2018) show an
510 estimated 24 Mm^3 of sediment dredged in the Ayeyarwady between 1989 and 2017, the
511 total volume of dredged material between 2012 and 2017 being 7.72 Mm^3 (about 12.4 Mt),
512 i.e., about one-third of the total volume dredged since 1989. Most of the dredging has
513 occurred since 2015 (78%), a year when 2.5 Mm^3 of material were removed from the river.
514 The dredging volumes are considerably lower than the estimated volumes of material
515 removed through sand and gravel mining, which are at least ten-fold higher, but they also
516 contribute to the aggravation of the sediment balance of the river. Although quantified
517 changes in the fluvial sediment load other than estimations of potential reservoir trapping,
518 aggregate extractions and dredging are still lacking (WWF, 2018), several activities in the
519 river catchment, notably mining (Fig. 10B) and agriculture, are currently generating massive
520 deforestation (Fig. 10C), which has been important in Myanmar in the recent decades
521 (Leimgruber et al., 2005; Hansen et al., 2013; Webb, 2013). Erosion of the bare slopes
522 generated by mining and deforestation is contributing to an increase in sediment supply to
523 the river system (WWF, 2018), thus counter-balancing the sediment reduction generated by
524 dams, in-channel mining and dredging.

525 Deltas need to keep up with sea-level rise and marine forcing. The chronic erosion
526 that affects the western sector of the delta (Fig. 6, 7) indicates, thus, that the sand supply to
527 the Ayeyarwady delta's shoreline is no longer sufficient to balance forcing. The shoreline is
528 deprived of sand needed to maintain its beaches by massive aggregate mining in the river
529 reaches (Fig. 10A) as well as by dams. The ensuing beach erosion occurs through both the
530 well acknowledged mechanism of diminished sand supply to inter-distributary beaches, and
531 the less well acknowledged effect of reversed (towards upstream) bedload transport in the
532 distributary mouths caused by salt intrusion resulting from artificial channel deepening

generated by aggregate extraction, as has been postulated for the Mekong delta (Anthony et al., 2015). In addition, the considerable amount of sediment stored in the river bed and fluvial floodplain as a result of rampant deforestation (Fig. 10C), could also be affected by the buffering of peak flows by reservoirs, causing reduction of the capacity for bedload mobilization towards the delta (WWF, 2018).

The narrowing beaches in the Ayeyarwady delta are being reworked, with landward migration through abundant washovers along the central sectors of beaches bounding the inter-distributary plains, accompanied by bi-directional drift that results in sand being stored in peripheral accreting spits (Anthony et al., 2017). This weakening of the delta's sandy 'armour' and the absence of aeolian dunes potentially favour massive landward translation of the high-water line during cyclones, as happened under the strong surge conditions generated by Cyclone Nargis in May 2008. The shoreline was translated landwards by hundreds of metres in places, resulting in weakening of, and lengthening of the time of, delta shoreline resilience as beach erosion became aggravated in the months following this event (Besset et al., 2017). This event was followed by slow recovery that has never been totally achieved in the dominantly erosional multi-decadal context in which these beaches now evolve.

An additional contributor to the erosion that affects the western sector of the delta could be sediment redistribution modulated by the numerous embankments built upstream in the fluvial reaches. The transport of sediment to the sea should, theoretically, be aided by river embankments, as such structures confine sediment within the channels and, thus, lower the spill-over of fluvial load onto the delta plain during the flood season (Woodroffe, 2000). Recognition of the loss of sediment from flooding for land in the delta led to a call for non-rebuilding of such embankments as early as 1939 (Kravtsova et al., 2009). However, while inhibiting lateral channel migration and deposition in the protected floodplain areas, these structures also enhance channel-bed aggradation, which exacerbates local flood hazard (Brakenridge et al., 2017) and reduces delivery of sediment to the coast. Over time, channel-bed sedimentation induces higher river levels for the same discharge (Pinter, 2005), with overbank flooding resulting in spillover of sediment onto the delta plain rather than sediment transport to the coast. The flood hazard and potential sequestering of bedload in the channel reaches are also exacerbated by the marked difference in slope between the main-stem Ayeyarwady and its various distributaries, all of which exhibit much steeper

565 slopes (WWF, 2018). This difference is deemed to be contributing to a glut in sediment in the
566 middle reaches well upstream of the delta, and the ensuing accumulation of sediment and
567 the river-bed aggradation exacerbate rainy season flooding (WWF, 2018).

568 The more sheltered eastern sector is, in contrast, the current main depocentre for
569 mud transported by coastal currents from the multiple mouths towards the Gulf of
570 Martaban (Fig. 3A). The overall trend indicated by the 10-year coastal SPM data (2002-2012)
571 from *GlobCoast* suggests that the fluvial fine-grained sediment supply exiting at the mouths
572 of the Ayeyarwady has been relatively stable overall (max $\pm$ 5%) (Fig. 11), assuming, of
573 course that these concentrations are a faithful reflection of fine-grained fluvial sediment
574 supply, which, as indicated earlier, seems to be the case. By balancing losses generated by
575 fine-grained sediment retention behind reservoirs, sediment released by deforestation could
576 explain the relative stability of the coastal SPM concentrations between 2002 and 2012 (Fig.
577 10), given the propensity for easier mobilization and transport of suspension load from the
578 fluvial reaches to the sea. This load largely dominates the sediment supply of the
579 Ayeyarwady (WWF, 2018), and has been dominant in the construction of the delta (Rodolfo,
580 1975). Another issue in the Ayeyarwady delta is that of aggravated subsidence (Syvitiski et
581 al., 2009), but the areal pattern of this process is not known. van der Horst et al. (2018) have
582 monitored very high local subsidence rates in Yangon (Fig. 1), Myanmar's capital city (5
583 million inhabitants), aggravated by urban development needs in terms of buildings,
584 infrastructure and ground-water abstraction. Tidal gauge data for the delta indicate a 3.4–6
585 mm/y relative sea-level rise (Syvitski et al., 2009). Aggravated subsidence and sea-level rise
586 can only be balanced by the trapping of more fine-grained sediment by the deltaic plain. An
587 increased supply of suspension load resulting from deforestation may essentially be
588 compensating for delta-plain subsidence, while also contributing to the current progradation
589 of the relatively sheltered eastern sector of the delta where sediment is trapped.

590 Significant losses of mangrove forests in the Ayeyarwady delta to shrimp farms and
591 rice fields, notably in the decade prior to Cyclone Nargis, have been identified (Hedley et al.,
592 2010; Frenken, 2012; Veettil et al., 2018; Chatagno et al., 2019). According to Hedley et al.
593 (2010), the total mangrove forest area decreased from 2345 km^2 to 1786 km^2 between 1924
594 and 1995 from clearance for agriculture and aquaculture. It is projected that unprotected
595 Ayeyarwady delta mangrove forests could be completely deforested by 2026 (Webb, 2013).
596 Chatagno (2019) mapped a loss of 636 km^2 of mangroves but also a much lower gain of 279

597 km^2 between 1998 and 2018, yielding a net loss of 29%. The contribution of mangrove loss
598 to shoreline change is hard to identify, since much of the erosion of the delta's shoreline
599 concerns the sandy beach sector in the west, where mangroves essentially occur in back-
600 barrier plains and fringe the delta distributary channels. If not controlled, mangrove removal
601 in the mud-dominated eastern sector of the delta could contribute to the local exacerbation
602 of erosion.
603
604 **6. Conclusion and perspectives**
605 Like many deltas worldwide, the Ayeyarwady deltas is faced with increasing
606 urbanization and investments in agriculture, fisheries and aquaculture, transport and
607 industry. But the river is also part of a large catchment in which issues of environment,
608 water management, climate change, economic and social development, and land use are
609 driving significant change (Taft and Evers, 2016), with strong implications for the sediment
610 balance of the delta. Irrigation and hydropower are going to be key elements of this
611 development (IFC, MOEE and MONREC, 2017), but could also pose a threat to the stability of
612 the Ayeyarwady delta. A considerable amount of sediment is reported to be stored in the
613 river bed and fluvial floodplain as a result of deforestation, such that the combined impact of
614 hydropower and irrigation dams will be more important, in the short term, in buffering peak
615 flows and thus reducing the capacity to move sediment to the delta, notably bedload, while
616 exacerbating the flood hazard (WWF, 2018). Future dams could only compound the
617 deleterious effects of existing reservoirs and of the current massive fluvial aggregate mining,
618 which, by curtailing sand supply to the coast, are the most important threat to the stability
619 of the delta's shoreline. In the future, the distributary mouths could be increasingly affected
620 by upstream bedload transport, and salt intrusion if aggregate extractions (and attendant
621 channel deepening) in the tidally-influenced reaches of the Ayeyarwady are maintained at
622 current levels. Unless such mining is regulated towards much more reasonable and less
623 damaging levels, and alternative solutions found to compensate for such regulation, the
624 sandy beaches of the delta will continue to recede, leading to impairing of their energy-
625 buffering capacity and their ability to protect large fronts of the delta. This could, in turn,
626 exacerbate the lowering of resilience to cyclones, thus increasing risks to humans and to the
627 delta ecosystem.
628

Acknowledgements

We thank WWF Asia for funding this project. Sami Tornikoski, Salai Thura Zaw, Hten Hten Thazen, and Htayla Aung of WWF Myanmar are thanked for their valuable support. Colin Woodroffe and another reviewer provided constructive suggestions for improvement.

References

ADB, 2012. Myanmar in transition: Opportunities and challenges. Asian Development Bank, Mandaluyong City, Philippines, 46 pp.

Anthony, E.J., 2015. Wave influence in the construction, shaping and destruction of river deltas: A review. Mar. Geol., 361, 53-78.

Anthony, E.J., 2016. River deltas. In: Oxford Bibliographies, Geoscience, Oxford University Press. **http://www.oxfordbibliographies.com/view/document/obo-9780199363445/obo-9780199363445-0057.xml?rskey=g50miF&result=1&q=Deltas#firstMatch.**

Anthony, E.J., Besset, M., Brunier, G., Goichot, M., Dussouillez, P., Nguyen, V.L., 2015. Linking rapid erosion of the Mekong River delta to human activities. Scientific Reports, 5, 14745.

Anthony, E.J., Besset, M., Dussouillez, P., 2017. Recent shoreline changes and morpho-sedimentary dynamics of the Ayeyarwady River delta: assessing the impact of anthropogenic activities on delta shoreline stability. Unpub. Report, WWF Asia and Helmsley Foundation, Yangon, Myanmar, 43 p.

Ashok, K., Guan, Z., Yamagata, T., 2001. Impact of the Indian Ocean dipole on the relationship between the Indian monsoon rainfall and ENSO. Geophys. Res. Lett. 28, 4499–4502.

Besset, M., Anthony, E.J., Bouchette, F., 2019a. Multi-decadal variations in delta shorelines and their relationship to river sediment supply: An assessment and review. Earth-Science Reviews, 193-199-219.

Besset, M., Anthony, E.J., Dussouillez, P., Goichot, M., 2017. The impact of Cyclone Nargis on the Ayeyarwady (Irrawaddy) River delta shoreline and nearshore zone (Myanmar): towards degraded delta resilience? Comptes Rendus Geoscience, 349, 238-247.

Besset, M., Gratiot, N., Anthony, E.J., Bouchette, F., Goichot, M., Marchesiello, P., 2019b. Mangroves and shoreline erosion in the Mekong River delta, Viet Nam. Estuarine, Coastal and Shelf Science, 226, 106263, https://doi.org/10.1016/j.ecss.2019.106263

660 Brakenridge, G.R., Syvitski, J.P.M., Niebuhr, E., Overeem, I., Higgins, S.A., Kettner, A.J.,
661 Prades, L., 2017. Design with nature: Causation and avoidance of catastrophic flooding,
662 Myanmar. Earth-Science Reviews 165, 81–109.
663 Brondizio, E.S., Foufoula-Georgiou, E., Szabo, S., Vogt, N., Sebesvari, Z., Renaud, F.G.,
664 Newton, A., Anthony, E.J., Mansur, A.V., Matthews, Z., Hetrick, S., Costa, S.M., Tessler, Z.,
665 Tejedor, A., Longjas, A., Dearing, J.A., 2016. Catalyzing action towards the sustainability of
666 deltas. Current Opinion in Environmental Sustainability. 19, 182-194.
667 Buurman, P., Van Lagen, B., Velthorst, E.J. (Eds.), 1996. Manual for Soil and Water Analysis,
668 Backhuys Publishers, Leiden, The Netherlands, pp. 314.
669 Chatagno, G., 2019. Evolution des forêts de mangroves dans les deltas tropicaux : causes et
670 conséquences. Master's dissertation (Year 1). Aix-Mareseille Univ., Aix en Provence, 52
671 pp.
672 Coleman, J.M., Huh, O.K., 2004. Major Deltas of the World: A Perspective from Space.
673 Coastal Studies Institute, Louisiana State University, Baton Rouge, LA, USA.
674 www.geol.lsu.edu/WDD/PUBLICATIONS/C&Hnasa04/C&Hfinal04.htm.
675 Damodararao, K., Singh, S.K., Rai, V.K., Ramaswamy, V., Rao, P.S., 2016. Lithology, monsoon
676 and sea-surface current control on provenance, dispersal and deposition of sediments
677 over the Andaman continental chelf. Front. Mar. Sci. 3:118. doi:
678 10.3389/fmars.2016.00118
679 Dube, S.K., Murty, T.S., Feyen, J.C., Cabrera, R., Harper, B.A., Bales, J.D., Amer, S. (Eds.),
680 2010. Storm surge modeling and applications in coastal areas. In: World Scientific Series
681 on Asia-Pacific Weather and Climate Global Perspectives on Tropical Cyclones Vol. 4.,
682 World Scientific Publishing, Singapore, p. 363–406.
683 Ericson, J.P., Vörösmarty, C.J., Dingman, S.L., Ward, L.G., Meybeck, M., 2006. Effective sea-
684 level rise and deltas: Causes of change and human dimension implications. Glob. Planet.
685 Chang. 50, 63-82.
686 Evans, G., 2012. Deltas: the fertile dustbins of the world. Proc. Geologist. Assoc., 123, 397–
687 418.
688 Frenken, K., 2012. Irrigation in Southern and Eastern Asia in figures, AQUASTAT Survey.
689 2011. FAO Water Reports 37. Food and Agriculture Organization of the UN, Rome, p. 487.
690 Fritz, H.M., Blount, C.D., Thwin, S., Thu, M.K., Chan, N., 2009. Cyclone Nargis storm surge in
691 Myanmar. Nat. Geosci. 2, 448–449.

692 Furuichi, T., Win, Z., Wasson, R.J., 2009. Discharge and suspended sediment transport in the
693 Ayeyarwady River, Myanmar: centennial and decadal changes. Hydrol. Process. 23, 1631–
694 1641.
695 Galloway, W.E., 1975. Process framework for describing the morphologic and stratigraphic
696 evolution of delta depositional systems. In: Broussard, M.L. (ed.), Deltas: Models for
697 Exploration. Texas Geological Society, Houston, pp. 87–98.
698 Garzanti, E., Wang, J., Vezzoli, G., Limonta, M., 2016. Provenance and sediment fluxes in the
699 Irrawaddy (Ayeyarwadi) River. Geophys. Res. Abstr. 18 EGU2016-1335, 2016, EGU
700 General Assembly, Vienna, 2016.
701 Giosan, L., Naing, T., Tun, M.M., Clift, P.D., Filip, F., Constantinescu, S., Khonde, N., Blusztajn,
702 J., Buylaert, P.J., Stevens, T., Thwin, S., 2018. On the Holocene evolution of the
703 Ayeyawady megadelta. Earth Surface Dynamics, 6, 451-466.
704 Grill, G., Lehner, B, Thieme, M., Geenen, B., Tickner, D., Antonelli, F., Babu, S., Borrelli, P.,
705 Cheng, L., Crochetiere, H., Ehalt Macedo, H., Filgueiras, R., Goichot, M., Higgins, J., Hogan,
706 Z., Lip, B., McClain, M. E., Meng, J., Mulligan, M., Nilsson, C., Olden, J. D., Opperman, J. J.,
707 Petry, P., Reidy Liermann, C., Sáenz, L., Salinas-Rodríguez, S., Schelle, P., Schmitt, R. J. P.,
708 Snider, J., Tan, F., Tockner, K., Valdujo, P. H., van Soesbergen, A., Zarfl, C., 2019. Mapping
709 the world's free-flowing rivers. Nature, 569, 215–221.
710 Hagenlocher, M., Renaud, F.G., Haas, S., Sebesvari, Z., 2018. Vulnerability and risk of deltaic
711 social-ecological systems exposed to multiple hazards. Science of the Total Environment,
712 631–632, 71–80.
713 Haggag, M., Yamashita, T., Kim, K.O., Lee, H.S., 2010. In: Charabi, Y. (Ed.), Indian Ocean
714 Tropical Cyclones and Climate. Springer Science and Business Media, pp. 73–82.
715 Han, B., Loisel, H., Vantrepotte, V., Mériaux, X., Bryère, P., Ouillon, S., Dessailly, D., Xing, Q,
716 Zhu, Q., 2016. Development of a semi-analytical algorithm for the retrieval of suspended
717 particulate matter from remote sensing over clear to very turbid waters. Remote Sens. 8,
718 211; doi:10.3390/rs8030211 2016.
719 Hansen, M. C., P. V. Potapov, R. Moore, M. Hancher, S. A. Turubanova, A. Tyukavina, D.
720 Thau, S. V. Stehman, S. J. Goetz, T. R. Loveland, A. Kommareddy, A. Egorov, L. Chini, C. O.
721 Justice, and J. R. G. Townshend. 2013. High-Resolution Global Maps of 21st-Century
722 Forest Cover Change. Science 342, 850–53.

Hedley, P.J., Bird, M.I., Robinson, R.A.J., 2010. Evolution of the Irrawaddy delta region since1850. Geogr. J. 176, 138–149.

Hendon, H.H., Salby, M.L., 1994. The life cycle of the Madden-Julian Oscillation. J. Atmos. Sci. 51, 2225–2237.

Hennig, T., 2016. Damming the transnational Ayeyarwady basin. Hydropower and the water-energy nexus. Renewable & Sustainable Energy Reviews, 65, 1232-1246.

Himmelstoss, E.A., Henderson, R.E., Kratzmann, M.G., and Farris, A.S., 2018. Digital Shoreline Analysis System (DSAS) version 5.0 user guide: U.S. Geological Survey Open-File Report 2018–1179, 110 p., https://doi.org/10.3133/ofr20181179.

IFC, MOEE and MONREC, 2017. Strategic Environmental Assessment (SEA) of the Hydropower Sector: Baseline Assessment Reports. Yangon and Nay Pyi Taw, Myanmar, 2017.

Jerolmack, D.J., 2009. Conceptual framework for assessing the response of delta channel networks to Holocene sea level rise. Quaternary Science Reviews 28: 1786-1800.

Kattelus, M., Rahaman, M. M., Varis, O., 2014. Myanmar under reform: Emerging pressures on water, energy and food security, Nat. Resour. Forum, 38, 85–98.

Kravtsova, V.I., Mikhailov, V.N., Kidyaeva, V.M., 2009. Hydrological regime,morphological features and natural territorial complexes of the Irrawaddy River Delta (Myanmar). Water Resources, 36, 259–276.

Krishnamurthy, V., Goswami, B.N., 2000. Indian monsoon—ENSO relationship on interdecadal timescale. J. Clim. 13, 579–595.

Kuehl, S., Williams, J., Liu, P., Harris, C., Day, W.A., Tarpley, D., Goodwyn, M., Yin, Y.A., 2019. Sediment dispersal and accumulation off the Ayeyarwady delta – tectonic and oceanographic controls. Mar. Geol., in press.

Leimgruber, P., Kelly, D.S., Steinninger, M.K., Brunner, J., Mueller, T., Songer, M., 2005. Forest cover change patterns in Myanmar (Burma) 1990–2000. Environ. Conserv., 32, 356-364.

Loisel, H., Vantrepotte, V., Dessailly, D., Steinmetz, F., Ramon, D., Han, B., Mériaux, X., Ouillon, S., Cauvin, A., Jamet, C., 2016. Suspended particulate matter variability of the global coastal waters over the MERIS time period. Ocean Optics XXIII (Vancouver, Canada), 23-28 Octobre, 2016.

754 Matamin, A.R., Ahmad, F., Mamat, M., Abdullah, K., Harun, S., 2015. Remote sensing of
755 suspended sediment over Gulf of Martaban. Ekologia, 34, 54-64.
756 Myanmar Irrigation Works Department, 2004. Irrigation works in Myanmar. (www.
757 irrigation.gov.mm/water/potentialwater resources.html).
758 Pekel, J.-F., Cottam, A., Gorelick, N., Belward, A.S., 2016. High-resolution mapping of global
759 surface water and its long-term changes. Nature, 540, 418–422.
760 Pinter, N., 2005. One step forward, two steps back on U.S. floodplains. Science, 308, 207–
761 208.
762 Ramaswamy, V., Rao, P.S., Rao, K.H., Thwin Swe, Srinivasa Rao, N., Raiker, V. 2004 Tidal
763 influence on suspended sediment distribution and dispersal in the northern Andaman Sea
764 and Gulf of Martaban. Mar. Geol., 208, 33–42.
765 Rao, P.S., Ramaswamy, V., Thwin Swe, 2005. Sediment distribution and transport on the
766 Ayeyarwady continental shelf, Andaman Sea. Mar. Geol., 216, 239–47.
767 Robinson, R.A.J., Bird, M.I., Oo, N.W., Hoey, T.B., Aye, M.M., Higgitt, D.L., X., LX., Swe, A.,
768 Tun, T., Win, S.L., 2007. The Irrawaddy River sediment flux to the Indian Ocean: the
769 original nineteenth-century data revisited. J. Geol. 115 (6), 629–640.
770 Rodolfo, K.S., 1969a. Sediments of the Andaman Basin, northeastern Indian Ocean. Mar.
771 Geol., 7, 371–402.
772 Rodolfo, K.S., 1969b. Bathymetry and marine geology of the Andaman Basin, and tectonic
773 implications for Southeast Asia. Geol. Soc. Am. Bull. 80, 1203–1230.
774 Rodolfo, K.S., 1975. The Irrawaddy Delta: Tertiary setting and modern offshore
775 sedimentation. In: Broussard, M.L. (ed.), *Deltas, Models for Exploration*. Houston
776 Geological Society, Houston, pp. 329-348.
777 Rojas, O., Li, Y., Cumani, R., 2014. Understanding the Drought Impact of El Niño on the
778 Global Agricultural Areas: An Assessment Using FAO's Agricultural Stress Index (ASI). Food
779 and Agriculture Organization of the United Nations, Rome.
780 Seijger, C., Douven, W. van Halsema, G., Hermans, L., Evers, J., Phi, H.L., Khan, M.F., Brunner,
781 J., Pols, L., Ligtvoet, W., Koole, S., Slager, K., Vermoolen, M.S., Hasan, S., Hoang, V.T.,
782 2016. An analytical framework for strategic delta planning: negotiating consent for long-
783 term sustainable delta development. J. Environ. Manage. 60, 1485-1509.

784 Sein, Z.M.M., Ogwang, B.A., Ongoma, V., Ogou, F.K., Batebana, K., 2015. Inter-annual
785 variability of summer monsoon rainfall overMyanmar in relation to IOD and ENSO.
786 Journal of Environmental and Agric. Sci., 4, 28–36.
787 Shimozono, T., Tajima, Y., Akamatsu, S., Matsuba, Y., Kawasaki, A., 2019. Large-scale channel
788 migration in the Sittang River estuary. Sci. Rep., 9, 9862.
789 Stamp, L. D., 1940. The Irrawaddy River. Geographical Journal, 95, 329-356.
790 Steinmetz, F., Deschamps, P.-Y., Ramon, D., 2011. Atmospheric correction in presence of sun
791 glint: application to MERIS. Opt. Express 19, 9783-9800.
792 Suwannathatsa, S., Wongwises, P., Wannawong, W., 2012. Seasonal Currents in the Bay of
793 Bengal and Andaman Sea Revealed by Reprocessed Observations. International
794 Conference on Environment Science and Engineering IPCBEE vol.3 2, IACSIT Press,
795 Singapore.
796 Syvitski, J.P.M., Kettner, A.J., Overeem, I., Hutton, E.W.H., Hannon, M.T., Brakenridge, G.R.,
797 Day, J., Vorosmarty, C., Saito, Y., Giosan, L., Nicholls, R.J., 2009. Sinking deltas due to
798 human activities. Nat. Geosci. 2, 681–686.
799 Syvitski, J.P.M., Saito, Y., 2007. Morphodynamics of deltas under the influence of humans.
800 Glob. Planet. Chang., 57, 261–282.
801 Taft, L., Evers, M., 2016. A review of current and possible future human–water dynamics in
802 Myanmar's river basins. Hydrol. Earth Syst. Sci., 20, 4913–4928.
803 Tamura, T., Saito, Y., Nguyen, V.L., Ta, T.K.O., Bateman, M.D., Matsumoto, D., Yamashita, S.,
804 2012. Origin and evolution of interdistributary delta plains; insights from Mekong River
805 delta. Geology, 40, 303-306.
806 Thieler, R.E., Himmelstoss, E.A., Zichichi, J.L., Ergul, A., 2017. The digital shoreline analysis
807 system (DSAS) version 4.0, an ArcGIS extension for calculating shoreline change (ver. 4.4,
808 july 2017). U.S. Geological Survey Open-File Report. 2008–1278.
809 van der Horst, T., Rutten, M.M., van de Giesen, N.C., Hanssen, R.F., 2018. Monitoring land
810 subsidence in Yangon, Myanmar using Sentinel-1 persistent scatterer interferometry and
811 assessment of driving mechanisms. Remote Sensing of Environment, 217, 101-110.
812 van der Velden, J., 2015. Understanding the Dynamics of the Ayeyarwady River, Myanmar.
813 (MSc. Thesis). Utrecht University, p. 30.
814 Veettil, B.K., Pereira, S.F.R., Quang, N.X., 2018. Rapidly diminishing mangrove forests in
815 Myanmar (Burma): a review. Hydrobiologia, 822, 19-35.

816 Volker, A. 1966. The deltaic area of the Irrawaddy river in Burma. In: Scientific problems of
817 the humid tropical zone deltas and their implications. Proceedings of the Dacca
818 Symposium, UNESCO, p.373–9.
819 Wang, Y., Sieh, K., Tun, S.T., Lai, K.-Y., Myint, T., 2014. Active tectonics and earthquake
820 potential of the Myanmar region, J. Geophys. Res. Solid Earth, 119, 3767–3822,
821 doi:10.1002/2013JB010762.
822 Ward, P.J., Jongman, B., Sperna Weiland, F., Bouwman, A., van Beek, R., Bierkens, M.F.P.,
823 Ligtvoet, W., Winsemius, H.C., 2013. Assessing flood risk at the global scale: model setup,
824 results, and sensitivity. Environ. Res. Lett. 8, 10.
825 Winsemius, H.C., Van Beek, L.P.H., Jongman, B., Ward, P.J., Bouwman, A., 2013. A framework
826 for global river flood risk assessments. Hydrol. Earth Syst. Sci. 17, 1871–1892.
827 Woodroffe, C.D., 2000. Deltaic and estuarine environments and their late Quaternary
828 dynamics on the Sunda and Sahul shelves J. Asian Earth Sci., 18, 393–413.
829 WWF, 2018. *C1.13 - State of the Ayeyarwady Basin Report Package 3 – Sediments and*
830 *Geomorphology, Draft Final Report*. Worldwide Fund for Nature, Greater Mekong, 190
831 pp. http://www.airbm.org/the-ayeyarwady-state-of-the-basin-assessment-soba/
832
833
834
835
836
837

838 FIGURE CAPTIONS

839 Figure 1. Shaded-relief map showing the setting and main tributaries of the Ayeyarwardy
840 River delta.
841
842 Figure 2. 2016 Google earth image of the Ayeyarwady delta (A), and wave (B) and tidal (C)
843 characteristics. The delta has been divided into two main sectors, eastern and western. Red
844 dots along the shoreline show field sites visited during a reconnaissance survey in
845 November, 2016. The wave climate was culled from the ERA-Interim hindcast wave database
846 (1978-2016) generated by the ECMWF (European Centre for Medium-Range Weather
847 Forecasting) Wave Atmospheric Model, the M2 tidal amplitude map derived from the tide
848 and current prediction programme *WXTide32*© (Version 4.6), and the one-year tidal record
849 from the nearshore tide gauge the location of which is shown in Fig. 2A.

850 Figure 3. Monthly mean values of suspended particulate matter (2002-2012) off the mouths
851 of the Ayeyarwady delta and along the Andaman coast culled from the *GlobCoast* database
852 and obtained from MERIS sensor with POLYMER atmospheric corrections (Han et al., 2016)
853 (A), and monsoon-influenced water levels in the river at Pyay and Hinthada (Fig. 1) at the
854 apex of the delta (B). The SPM show high concentrations in June (start of the rainy season)
855 and December (dry season, reflecting, probably, a lag in terrestrial fine-grained sediment
856 supply to the coast following overbank sedimentation in the river flood plain and delta plain
857 during the rainy season which lasts till October).
858
859 Figure 4. Examples of mid-beach sand samples depicting alongshore variations in shoreline
860 sedimentology in the sandy, western sector of the Ayeyarwady delta (sites 8-17) and
861 transitional sandy-muddy shoreline (sites 6, 7) towards the mud-dominated eastern sector
862 (not shown here).
863
864 Figure 5. Ground photographs (November, 2016) of the two dominant shoreline types in the
865 Ayeyarwady: sandy beaches with muddy low-tide foreshores (A), and dominantly muddy
866 mangrove shorelines with local concentrations of sand (B), and sometimes colonized by
867 shore-front saltmarshes (foreground in B1).
868

Figure 6. Net shoreline mobility along the Ayeyarwady delta between April 1974 and April 2019. Erosion has dominated in the sandy western sector of the delta, whereas accretion has been preponderant in the eastern sector, with increased rates east of Yangon.

Figure 7. Coastal area change at different time frames between April 1974 and April 2019, highlighting both the accretion in the eastern sector that has gained momentum in 2015-2019, and the decreasing erosion trend in the western sector since 1988 and turnaround to very mild accretion since 2010, much of it explained by the area gains in the northeast portion of this sector between sites 7 and 10.

Figure 8. Massive local reworking of muddy foreshore deposits in the eastern sector of the delta close to the mouth of the Sittaung, where several mud banks have accumulated, reflecting the important mud storage and mud remobilisation in this part of the delta.

Figure 9. Map of land-water and water-land conversion of the coastal Ayeyarwady delta between 1984 and 2015 generated from data downloaded from Pekel et al. (2016), and percentages of various categories of conversion within a 2 km-wide coastal band. The coastal band shows the dominance (78%) of conversion of land into permanent or seasonal water, and of seasonal water into permanent water, largely indicative of shoreline erosion. Wetlands behind narrow beaches in this 2 km-wide band probably correspond to areas converted to rice cultivation, whereas small areas of water-to-land conversion correspond to accreting spits.

Figure 10. Summary of river-use and land-use pressures in the Ayeyarwady catchment that are affecting the sediment discharge (adapted from WWF, 2018), with impacts on sediment supply to the delta shoreline and its mobility. Massive aggregate extraction in the lower fluvial reaches of the Ayeyarwady and upper delta distributary channels is deemed to be leading to chronic erosion of the delta's sandy beaches in the western sector, whereas new sediment releases from deforestation caused by agriculture and mining may be contributing to the maintenance of sustained levels of suspended sediments that are mainly contributing to progradation of the muddy eastern sector of the delta.

Figure 11. Map of 10-year (2002-2012) overall evolution pattern of SPM concentrations (A), and monthly seasonal evolution trends (B) over the same period in the nearshore zone and over the continental shelf of the Ayeyarwady delta (data from *GlobCoast*, http://sextant.ifremer.fr/en/geoportail/sextant). The data show relatively stable concentrations over the ten-year period.

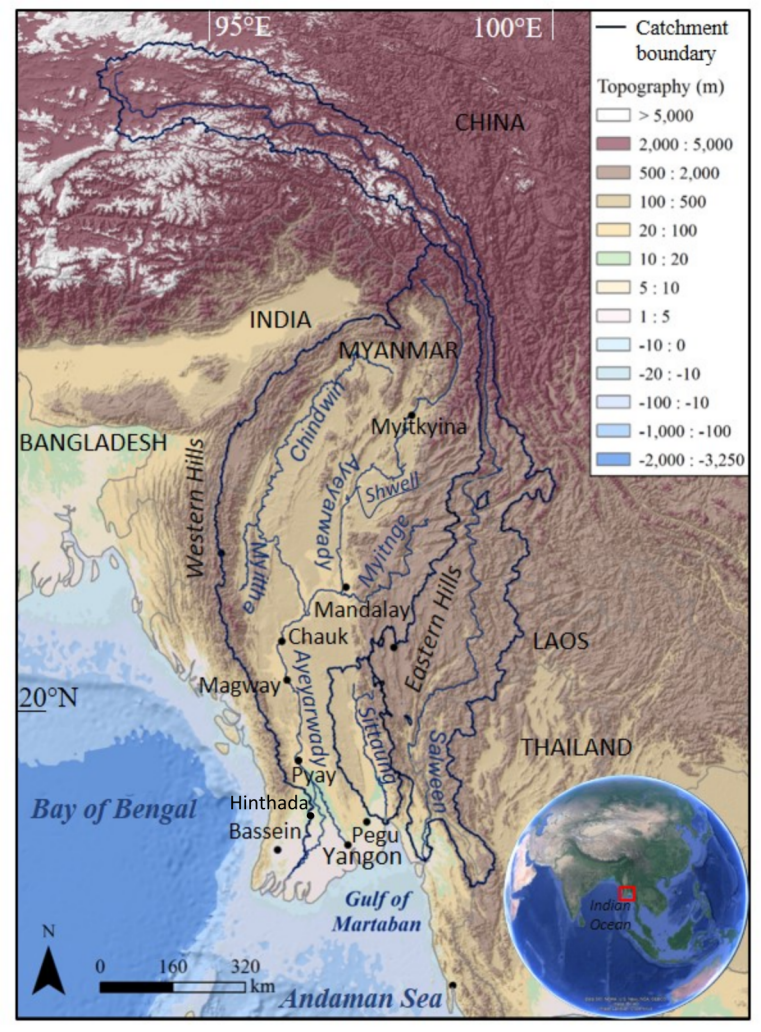
95°E
100°E
Catchment boundary
Topography (m)
> 5,000
2,000 : 5,000
500 : 2,000
100 : 500
20 : 100
10 : 20
5 : 10
1 : 5
-10 : 0
-20 : -10
-100 : -10
-1,000 : -100
-2,000 : -3,250
CHINA
INDIA
MYANMAR
BANGLADESH
LAOS
THAILAND
Myitkyina
Chindwin
Ayeyarwady
Shwell
Myitnge
Mandalay
Chauk
Magway
Pyay
Hinthada
Bassein
Pegu
Yangon
Western Hills
Eastern Hills
Sittaung
Saween
20°N
Bay of Bengal
Gulf of Martaban
Andaman Sea
Indian Ocean
N
0
160
320
km

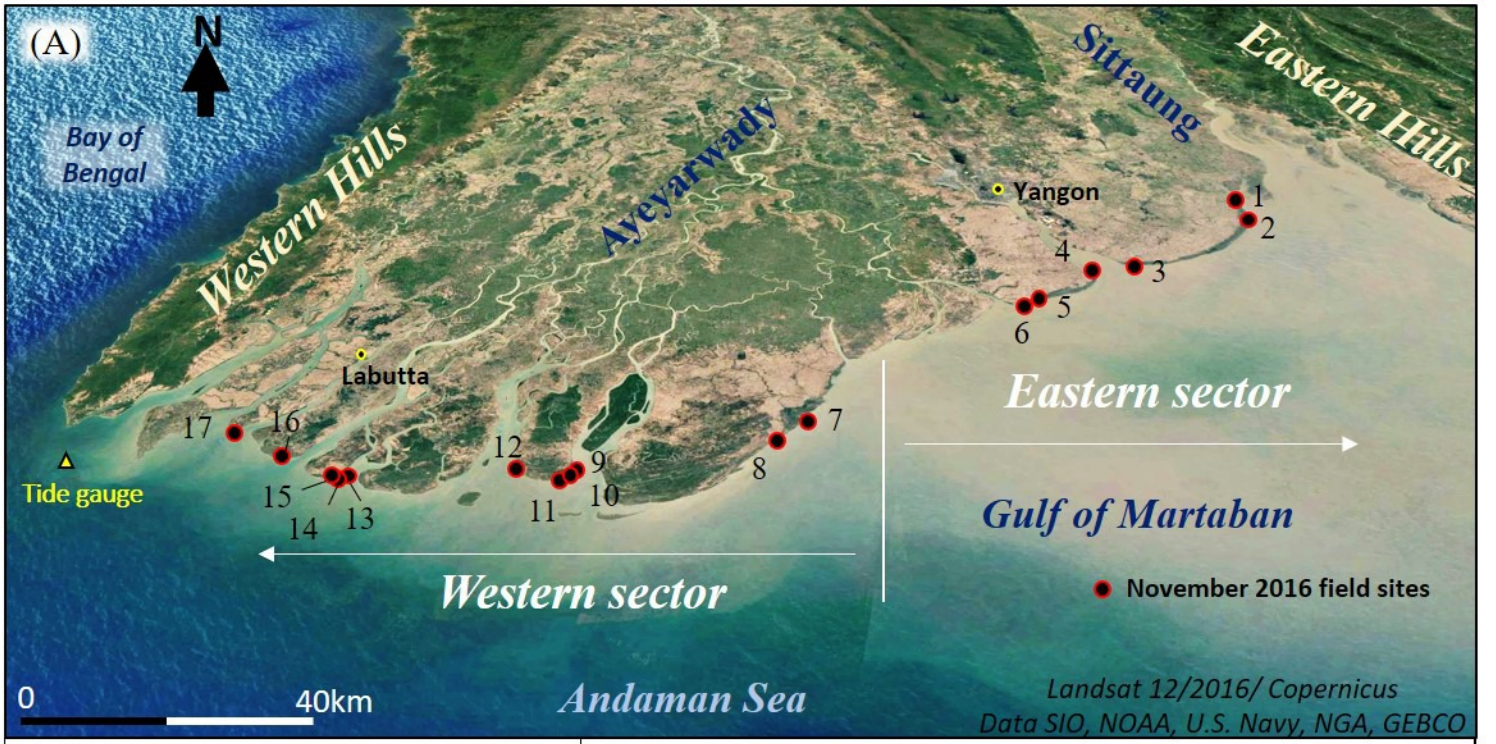
(A)
N
Bay of Bengal
Western Hills
Ayeyarwady
Sittaung
Eastern Hills
Yangon
Labutta
Tide gauge
Eastern sector
Gulf of Martaban
Western sector
November 2016 field sites
0
40km
Andaman Sea
Landsat 12/2016/ Copernicus
Data SIO, NOAA, U.S. Navy, NGA, GEBCO

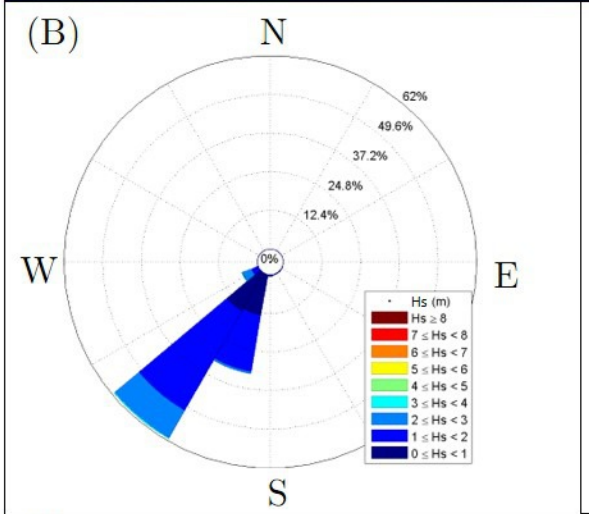
(B)
N
W
E
S
62%
49.6%
37.2%
24.8%
12.4%
0%
Hs (m)
Hs ≥ 8
7 ≤ Hs < 8
6 ≤ Hs < 7
5 ≤ Hs < 6
4 ≤ Hs < 5
3 ≤ Hs < 4
2 ≤ Hs < 3
1 ≤ Hs < 2
0 ≤ Hs < 1

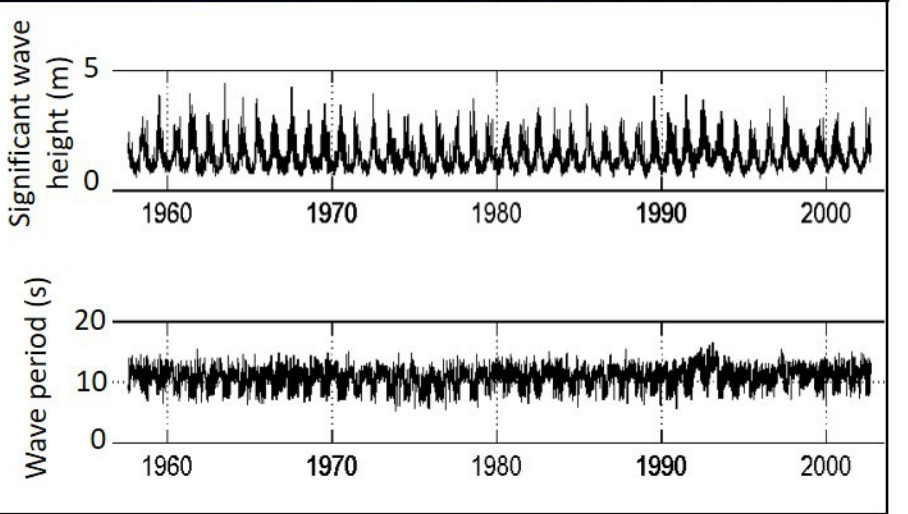
Significant wave height (m)
5
0
1960
1970
1980
1990
2000
Wave period (s)
20
10
0
1960
1970
1980
1990
2000

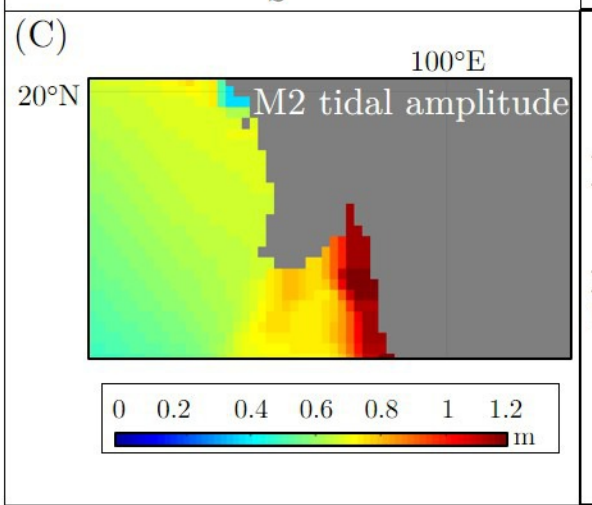
(C)
100°E
20°N
M2 tidal amplitude
0 0.2 0.4 0.6 0.8 1 1.2
m

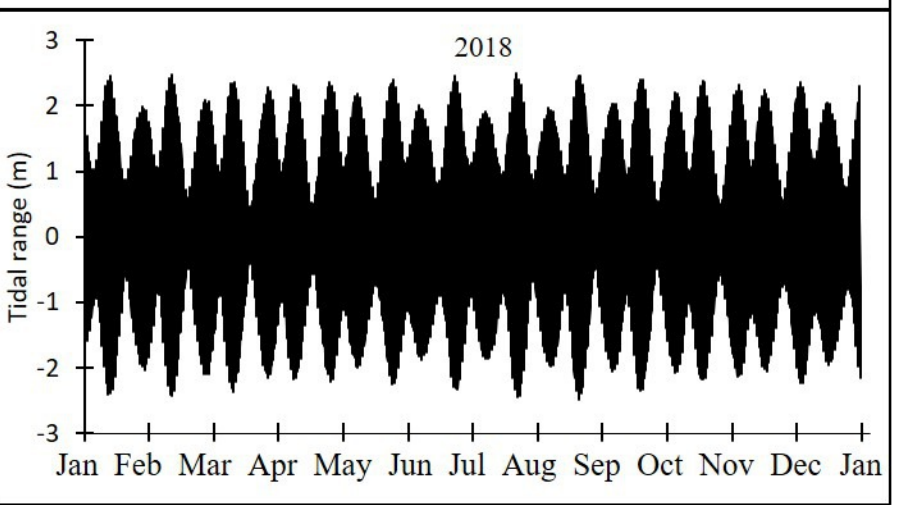
2018
Tidal range (m)
3
2
1
0
-1
-2
-3
Jan Feb Mar Apr May Jun Jul Aug Sep Oct Nov Dec Jan

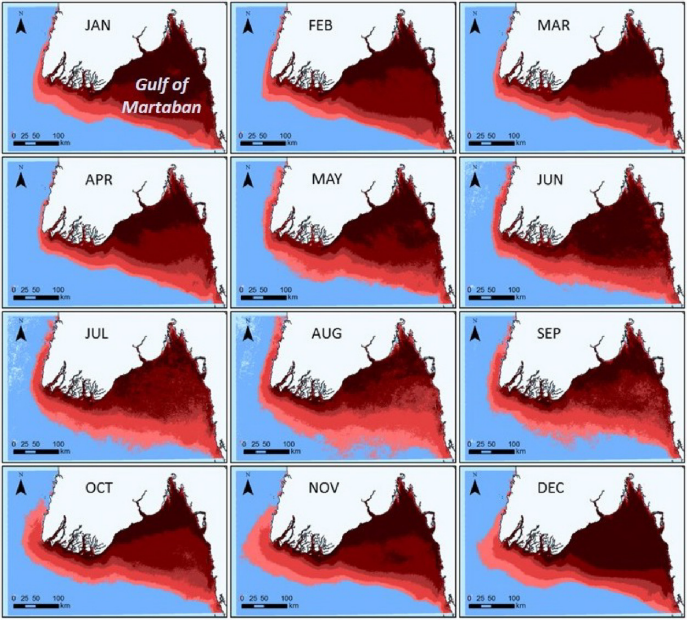

(A) - Concentrations in suspended particulate matter (g/m^3)

- > 200
- 100 : 200
- 50 : 100
- 10 : 50
- 5 : 10
- 1 : 5
- 0.1 : 1

(B) - Water levels at Pyay and Hinthada, 2015

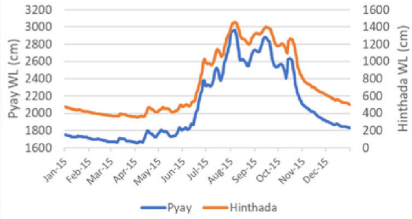

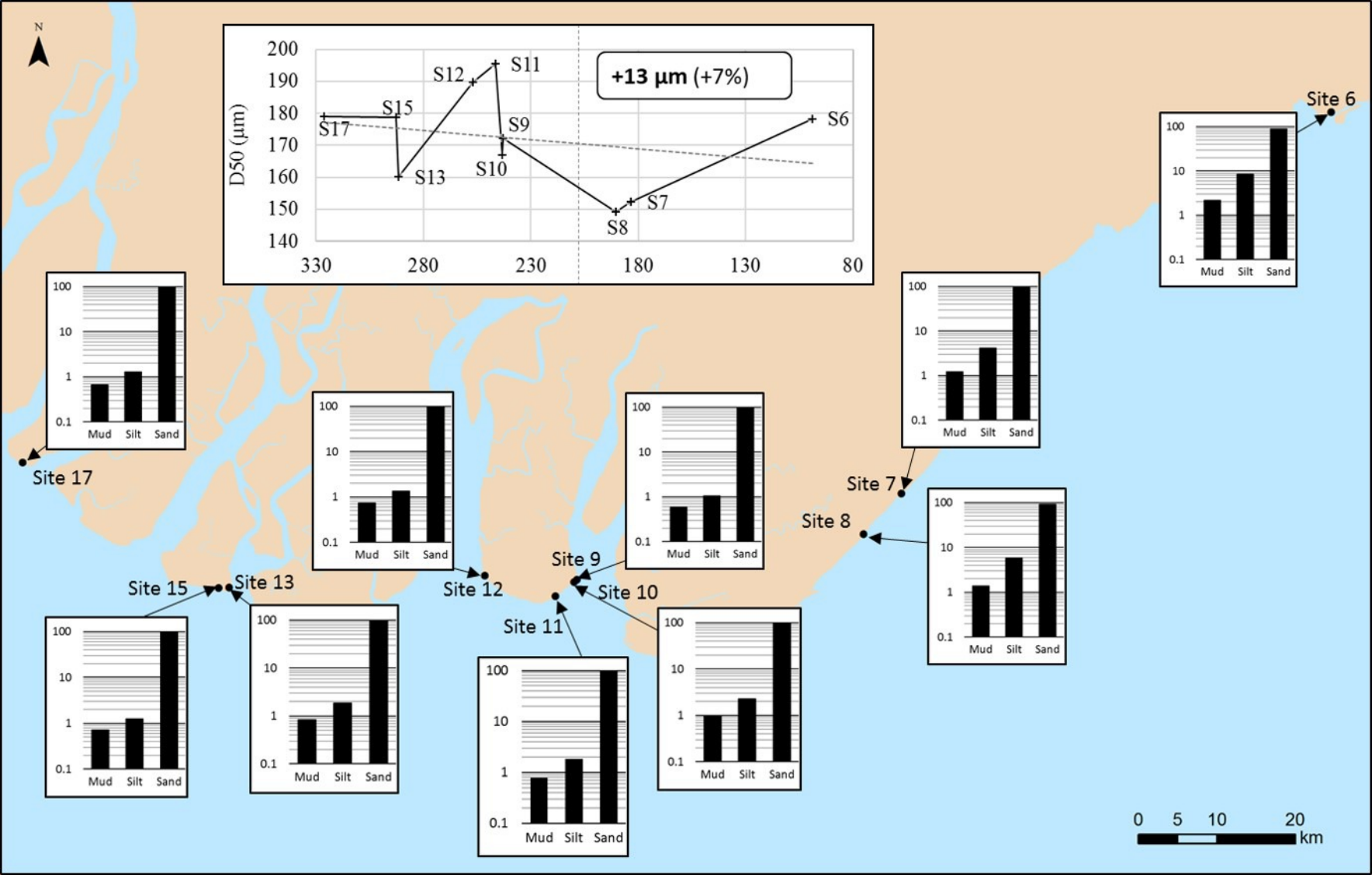
N
D50 (µm)
200
190
180
170
160
150
140
330
280
230
180
130
80
S17
S15
S12
S11
S13
S10
S9
S8
S7
S6
+13 µm (+7%)
Site 6
Site 17
Site 7
Site 8
Site 9
Site 10
Site 11
Site 12
Site 13
Site 15
100
10
1
0.1
Mud
Silt
Sand
0
5
10
20
km


(A1)
(B1)
(A2)
(B2)

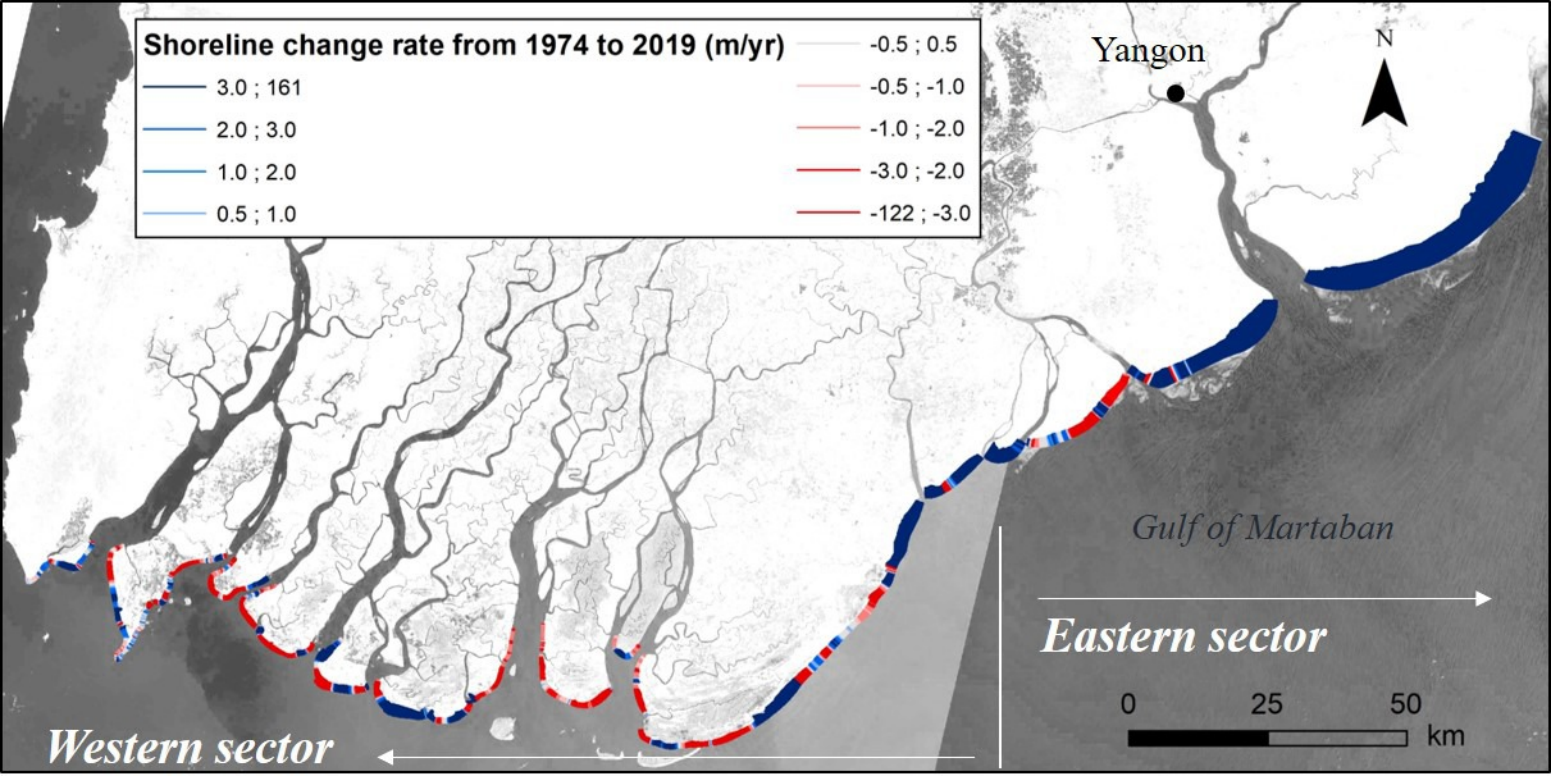
Shoreline change rate from 1974 to 2019 (m/yr)
3.0 ; 161
2.0 ; 3.0
1.0 ; 2.0
0.5 ; 1.0
-0.5 ; 0.5
-0.5 ; -1.0
-1.0 ; -2.0
-3.0 ; -2.0
-122 ; -3.0
Yangon
N
Gulf of Martaban
Eastern sector
Western sector
0
25
50
km

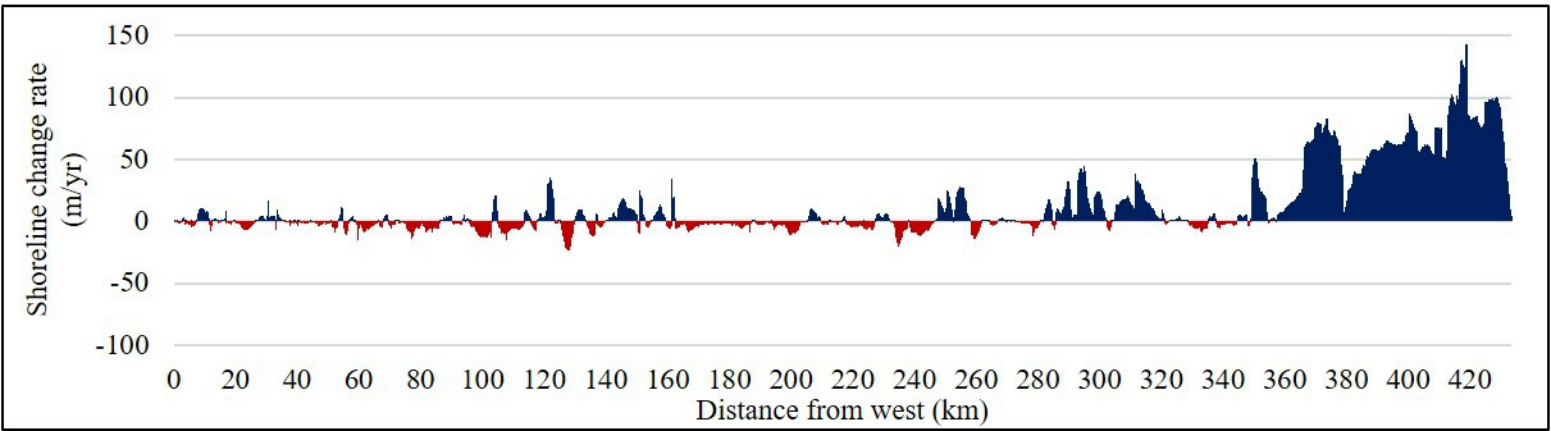
Shoreline change rate (m/yr)
150
100
50
0
-50
-100
0
20
40
60
80
100
120
140
160
180
200
220
240
260
280
300
320
340
360
380
400
420
Distance from west (km)

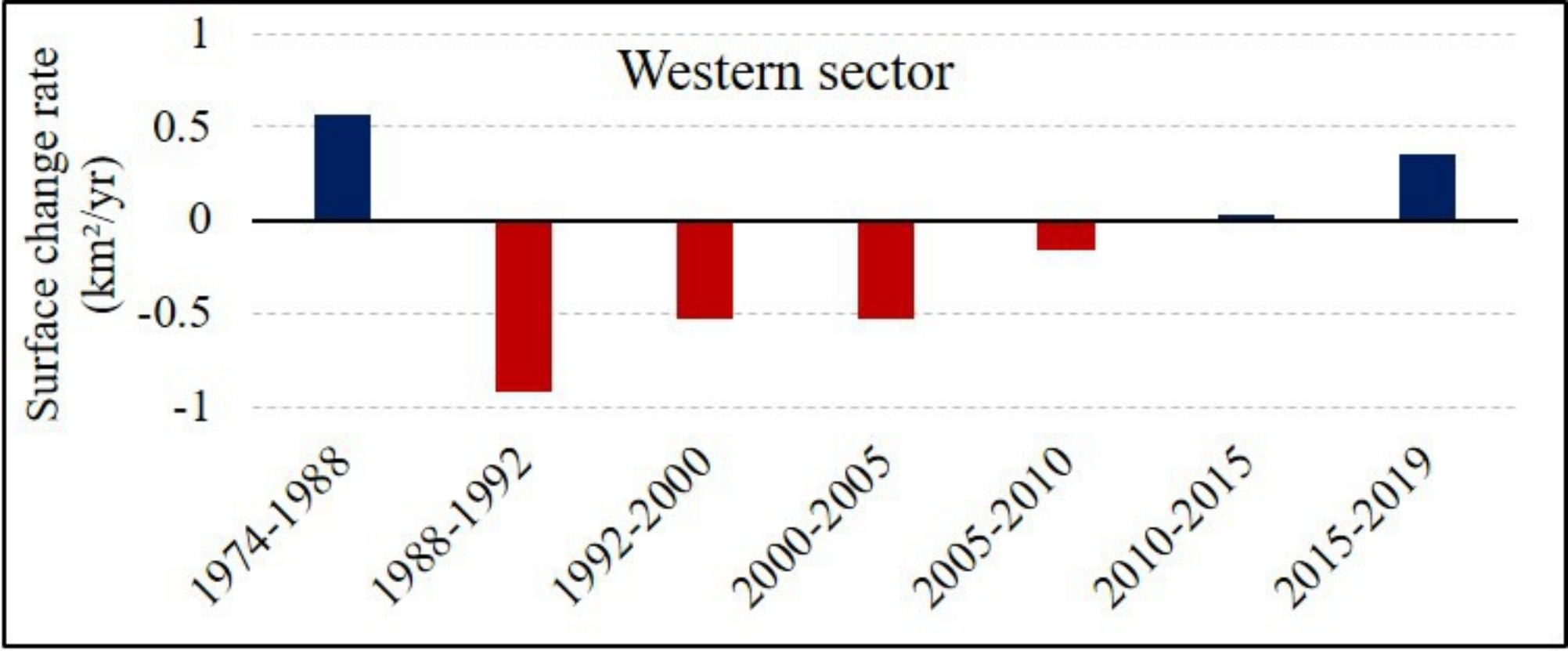
Western sector
Surface change rate (km²/yr)
1
0.5
0
-0.5
-1
1974-1988
1988-1992
1992-2000
2000-2005
2005-2010
2010-2015
2015-2019

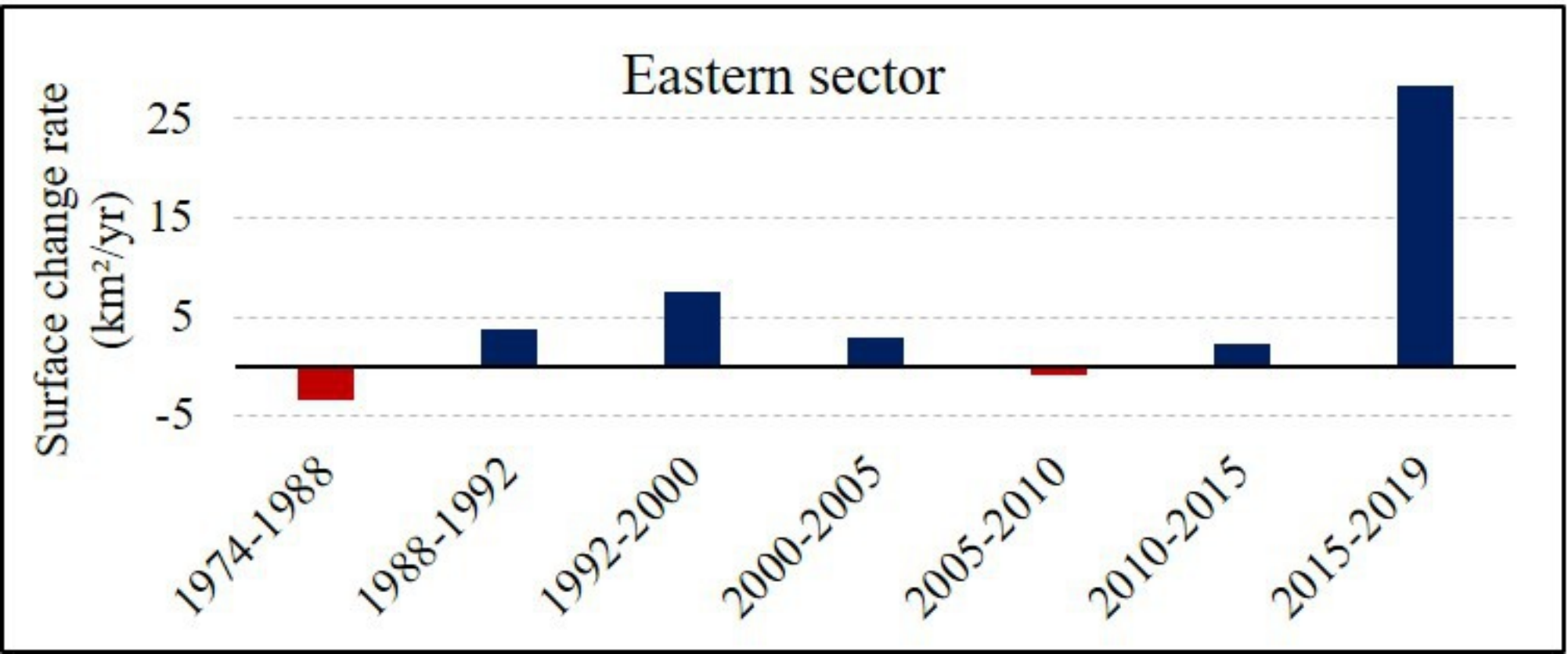
Eastern sector
Surface change rate (km²/yr)
25
15
5
-5
1974-1988
1988-1992
1992-2000
2000-2005
2005-2010
2010-2015
2015-2019

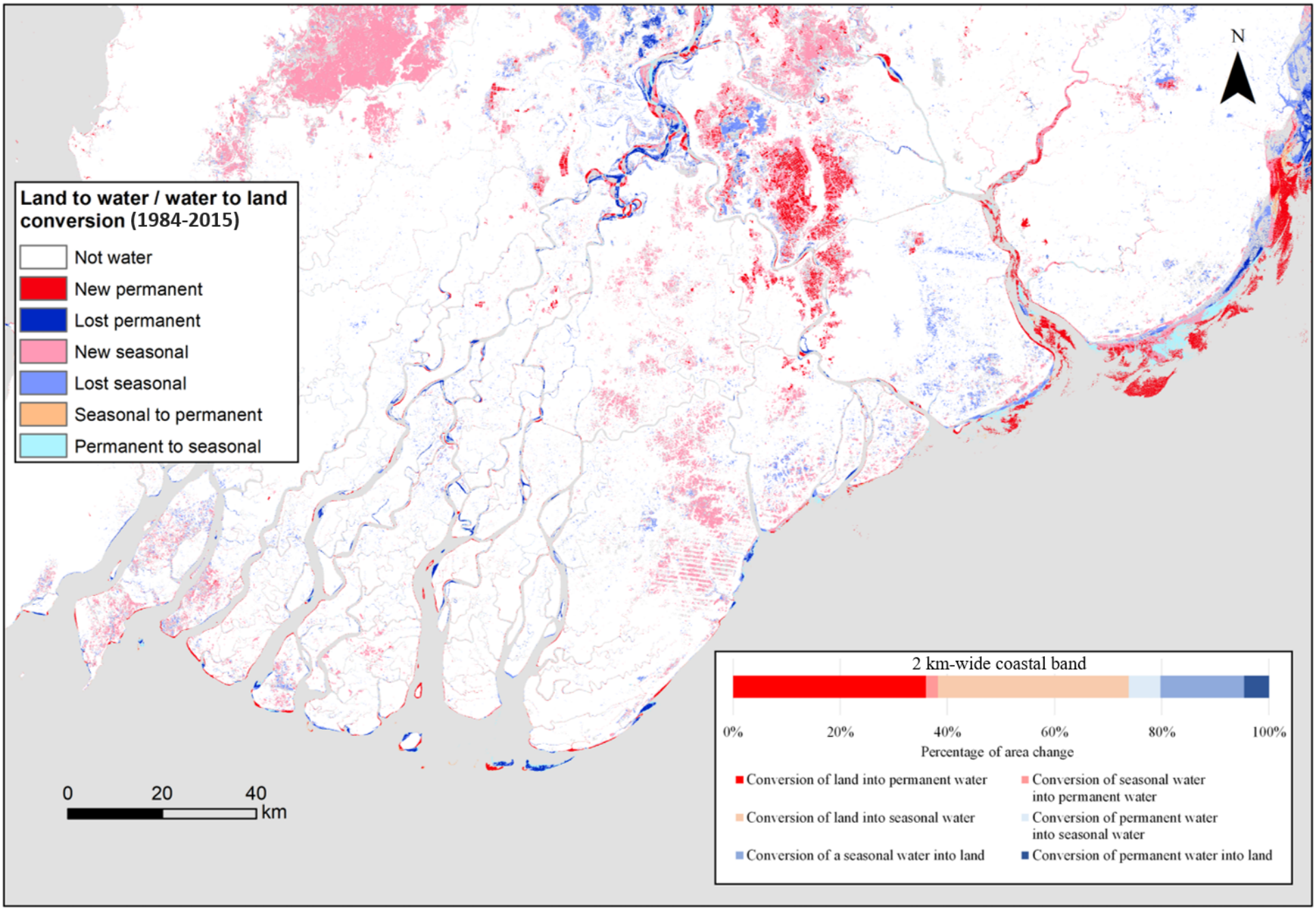
Land to water / water to land conversion (1984-2015)
Not water
New permanent
Lost permanent
New seasonal
Lost seasonal
Seasonal to permanent
Permanent to seasonal
N
0
20
40
km
2 km-wide coastal band
0%
20%
40%
60%
80%
100%
Percentage of area change
Conversion of land into permanent water
Conversion of seasonal water into permanent water
Conversion of land into seasonal water
Conversion of permanent water into seasonal water
Conversion of a seasonal water into land
Conversion of permanent water into land

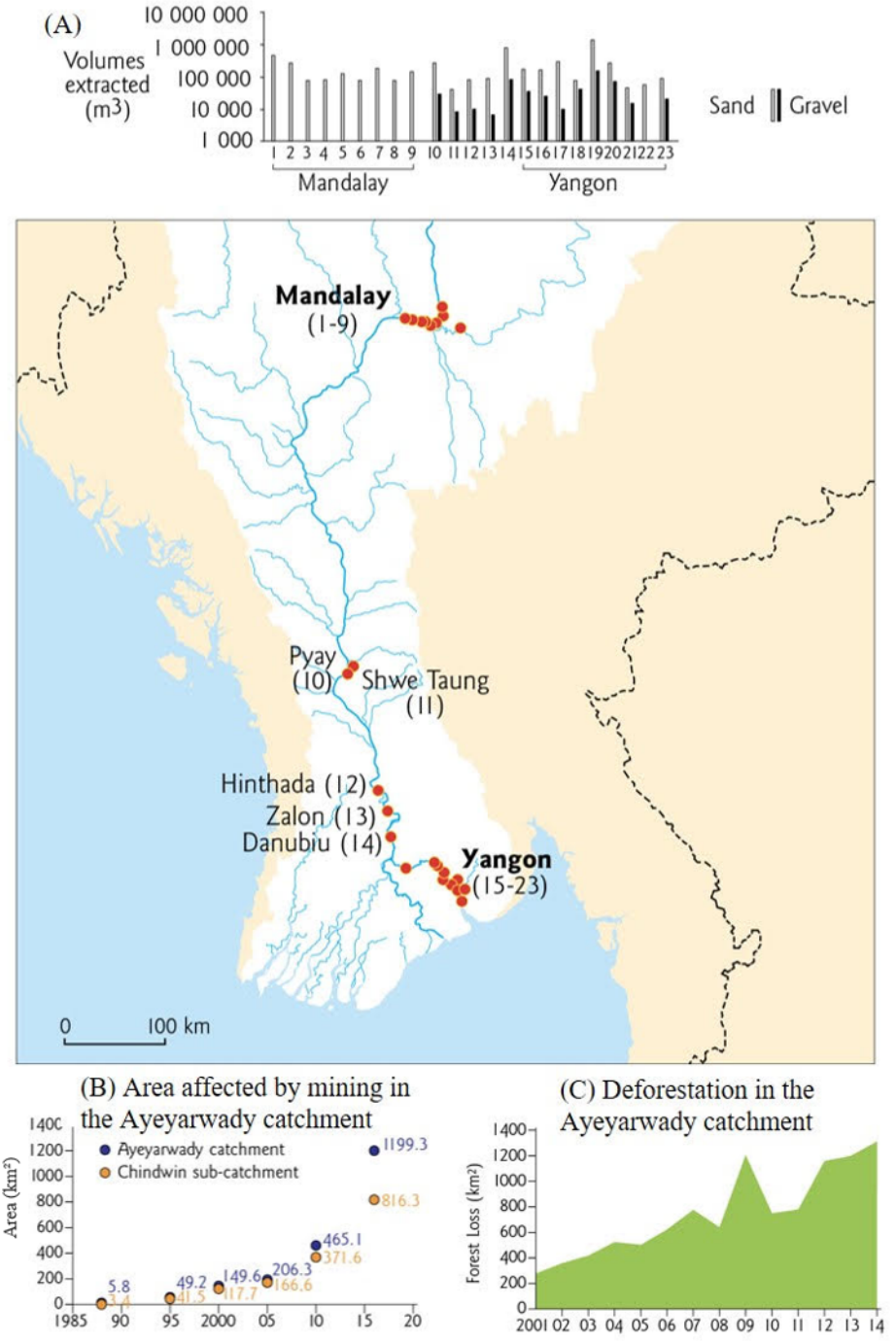
(A)
Volumes extracted (m3)
10 000 000
1 000 000
100 000
10 000
1 000
1 2 3 4 5 6 7 8 9 10 11 12 13 14 15 16 17 18 19 20 21 22 23
Mandalay
Yangon
Sand
Gravel
Mandalay (1-9)
Pyay (10)
Shwe Taung (11)
Hinthada (12)
Zalon (13)
Danubiu (14)
Yangon (15-23)
0
100 km
(B) Area affected by mining in the Ayeyarwady catchment
Area (km²)
Ayeyarwady catchment
Chindwin sub-catchment
1400
1200
1000
800
600
400
200
0
1985 90 95 2000 05 10 15 20
5.8
3.4
49.2
41.5
149.6
117.7
206.3
166.6
465.1
371.6
1199.3
816.3
(C) Deforestation in the Ayeyarwady catchment
Forest Loss (km²)
1400
1200
1000
800
600
400
200
0
2001 02 03 04 05 06 07 08 09 10 11 12 13 14

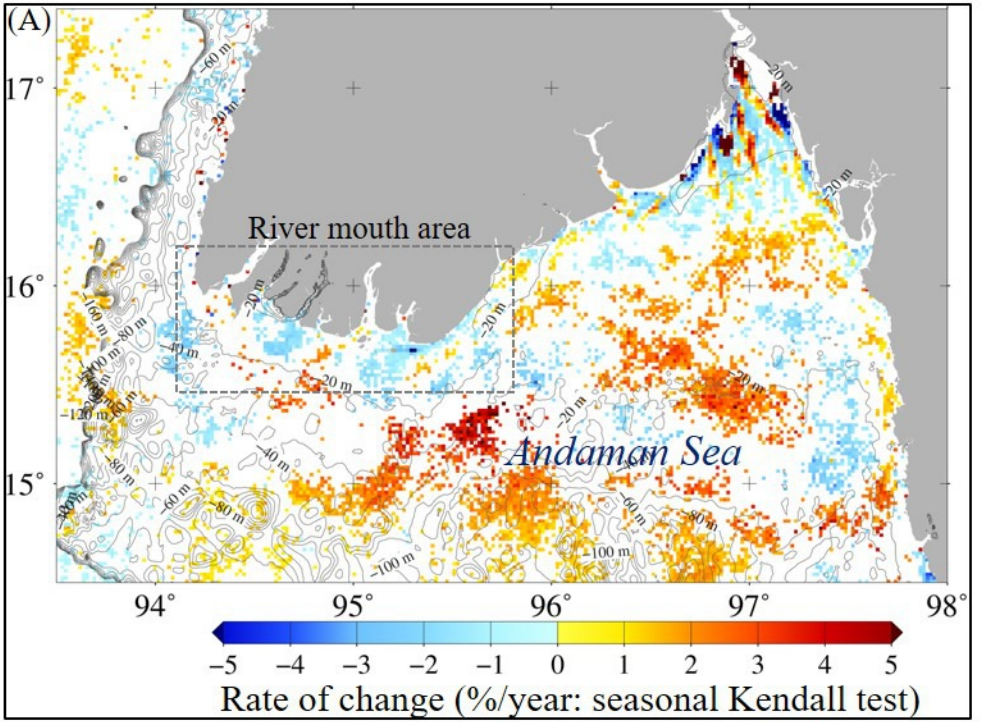
(A)
17°
16°
15°
94°
95°
96°
97°
98°
River mouth area
Andaman Sea
−5 −4 −3 −2 −1 0 1 2 3 4 5
Rate of change (%/year: seasonal Kendall test)

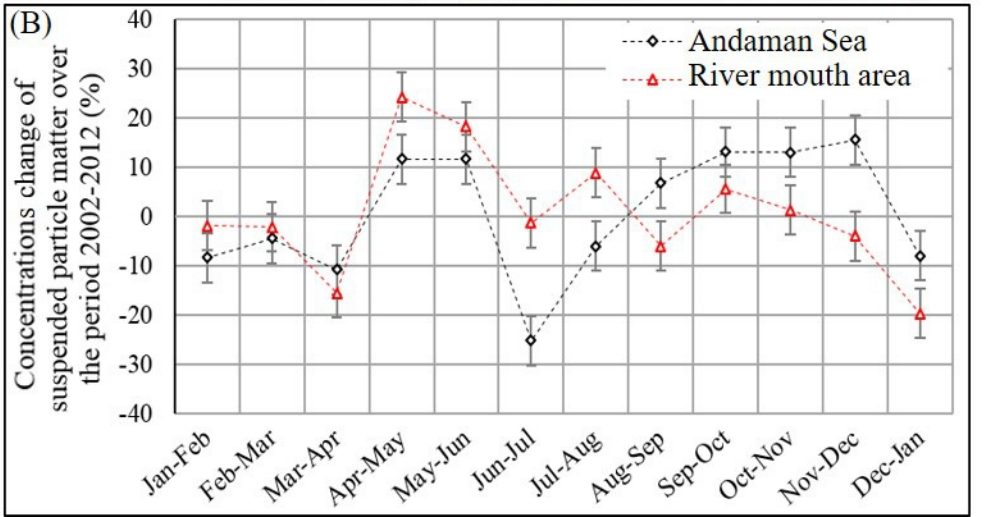
(B)
Concentrations change of suspended particle matter over the period 2002-2012 (%)
40
30
20
10
0
-10
-20
-30
-40
Andaman Sea
River mouth area
Jan-Feb
Feb-Mar
Mar-Apr
Apr-May
May-Jun
Jun-Jul
Jul-Aug
Aug-Sep
Sep-Oct
Oct-Nov
Nov-Dec
Dec-Jan